arXiv:2509.00895v1 [math.OC] 31 Aug 2025

# Sharp-Peak Functions for Exactly Penalizing Binary Integer Programming*

Shenglong Zhou† Shuai Li† Hui Zhang‡ Ziyan Luo†§

**Abstract:** Unconstrained binary integer programming (UBIP) is a challenging optimization problem due to the presence of binary variables. To address the challenge, we introduce a novel class of functions named sharp-peak functions (SPFs), which equivalently reformulate the binary constraints as equality constraints, giving rise to an SPF-constrained optimization. Rather than solving this constrained reformulation directly, we focus on its associated penalty model. The established exact penalty theory shows that the global minimizers of UBIP and the penalty model coincide when the penalty parameter exceeds a threshold, a constant independent of the solution set of UBIP. To analyze the penalty model, we introduce Karush-Kuhn-Tucker (KKT) points and a new type of stationarity, referred to as P-stationarity, and provide a comprehensive characterization of its optimality conditions. We then develop an efficient algorithm called ShaPeak based on the inexact alternating direction methods of multipliers, which is guaranteed to converge to a P-stationary point at a linear rate under appropriate parameter choices and a single mild assumption, namely, the local Lipschitz continuity of the gradient over a bounded box. Finally, numerical experiments demonstrate the high performance of ShaPeak in comparison to several established solvers.

**Keywords**: UBIP, Sharp-peak functions, exact penalty theory, P-stationary points, global convergence, linear convergence rate

## 1 Introduction

Binary integer programming (BIP) is a fundamental optimization problem with extensive applications across various domains, such as classical problems like the knapsack problem [2, 20] in combinatorial optimization and the max-cut problem [5, 37] in graph-based optimization. It has also attracted significant attention in modern machine learning, including adversarial attacks [9, 33], transductive inference [14], and binary neural networks [17, 25]. For additional applications, we refer to [18, 24]. The unconstrained version of BIP is given by

$$\min_{\mathbf{x}\in\mathbb{R}^n} \ f(\mathbf{x}), \quad \text{s.t.} \ \ \mathbf{x}\in\{0,1\}^n, \tag{UBIP}$$

where function $f:\mathbb{R}^n\to\mathbb{R}\cup\{\infty\}$ is continuously differentiable. However, UBIP is well-recognized as an NP-hard problem due to the presence of binary variables [10, 15]. Instead of directly solving (UBIP), we aim to address the following sharp-peak function constrained optimization (SPCO),

$$\min_{x\in\mathbb{R}^n} \ f(\mathbf{x}), \quad \text{s.t.} \ \ g(x_i)=0, \ 0\leqslant x_i\leqslant 1, \ i\in[n], \tag{SPCO}$$

where $[n]:=\{1,2,\cdots,n\}$ and $g:\mathbb{R}\to\mathbb{R}\cup\{\infty\}$ is a sharp-peak function as outlined in Definition 2.1. In general, for any $x\in[0,1]$, it satisfies $g(x)\geqslant 0$ and $g(x)=0$ if and only if $x\in\{0,1\}$.

*This work is supported by the National Key R&D Program of China (No. 2023YFA1011100).

†School of Mathematics and Statistics, Beijing Jiaotong University, China.
‡School of Management Science, Qufu Normal University, China.
§Email: shlzhou@bjtu.edu.cn, 24110488@bjtu.edu.cn, zhanghuiopt@163.com, luozy@bjtu.edu.cn

Table 1: Main techniques to process the binary constraints.

| Methods | References | Reformulations |
|---|---|---|
| | Relaxation methods | |
| LP relaxation | [12, 16] | $\{0,1\}^n \approx \{\mathbf{x} \mid 0 \leqslant \mathbf{x} \leqslant 1\}$ |
| Spectral relaxation | [7, 29] | $\{0,1\}^n \approx \left\{\mathbf{x} \mid \|2\mathbf{x}-1\|_2^2 = n\right\}$ |
| SDP relaxation | [3, 32] | $\{0,1\}^n \approx \left\{\mathbf{x} \mid \mathbf{X} \succeq \mathbf{x}\mathbf{x}^\top, \mathrm{diag}(\mathbf{X}) = \mathbf{x}\right\}$ |
| Doubly positive relaxation | [13, 34] | $\{0,1\}^n \approx \left\{\mathbf{x} \mid \mathbf{X} \succeq (2\mathbf{x}-1)(2\mathbf{x}-1)^\top, \mathrm{diag}(\mathbf{X}) = 1\right\}$ |
| | Equivalent reformulations | |
| Piecewise | [40] | $\{0,1\}^n \Leftrightarrow \{\mathbf{x} \mid \mathbf{x} \odot (1-\mathbf{x}) = 0\}$ |
| $\ell_2$ box | [22, 26] | $\{0,1\}^n \Leftrightarrow \left\{\mathbf{x} \mid 0 \leqslant \mathbf{x} \leqslant 1, \|2\mathbf{x}-1\|_2^2 = n\right\}$ |
| $\ell_2$ box MPEC | [39] | $\{0,1\}^n \Leftrightarrow \left\{\mathbf{x} \mid 0 \leqslant \mathbf{x} \leqslant 1, \|\mathbf{v}\|^2 \leqslant n, \langle 2\mathbf{x}-1, \mathbf{v}\rangle = n\right\}$ |
| $\ell_p$ box $(p > 0)$ | [36] | $\{0,1\}^n \Leftrightarrow \{\mathbf{x} \mid 0 \leqslant \mathbf{x} \leqslant 1, \|2\mathbf{x}-1\|_p^p = n, p > 0\}$ |
| $\ell_0$ norm | [38] | $\{0,1\}^n \Leftrightarrow \{\mathbf{x} \mid \|\mathbf{x}\|_0 + \|\mathbf{x}-1\|_0 \leqslant n\}$ |
| SPF | This paper | $\{0,1\}^n \Leftrightarrow \{\mathbf{x} \mid 0 \leqslant \mathbf{x} \leqslant 1, g_i(\mathbf{x}) = 0, i \in [n]\}$ |

### 1.1 Related work

Strategies for handling binary constraints can broadly be classified into two categories: relaxation methods and equivalent reformulations, see Table 1. We provide a brief overview below.

Relaxation methods aim to convert binary constraints into continuous optimization models, making them more tractable. One standard approach was linear programming relaxation [12, 16], where the binary constraint was replaced by a box constraint. This transformation turned the original NP-hard problem into a convex optimization problem with box constraints, which can be solved efficiently using modern optimization algorithms. Further advancements include spectral relaxation [7, 29], which substituted the binary constraint with a spherical constraint. The resulting problem is then solved through eigenvalue decomposition. Another notable contribution relaxed the binary constraint by a convex cone to derive the semi-definite programming (SDP) formulations. Then these SDP can be solved by some customized algorithms, such as interior point methods [35, 1], quasi-Newton and smoothing Newton methods [32], a spectral bundle method [11], branch-and-bound algorithms [4, 3]. To refine the relaxation, a doubly positive relaxation method [13, 34] enforced non-negativity constraints on both the eigenvalues and the elements of the SDP solution. Numerical results have demonstrated that this approach can significantly improve the solution quality compared to traditional SDP relaxation methods.

Equivalent reformulations provide another approach to addressing binary constraints in optimization problems. For example, a piecewise constraint was introduced in [40] to transform the UBIP into an equality-constrained optimization problem, which can be tackled using penalty methods. Similarly, the authors in [26] reformulated the UBIP as a continuous optimization problem using the $l_2$ norm, allowing it to be solved with second-order interior-point methods [8, 22]. Then this approach has been extended by [39], where the authors incorporated $l_2$ norm within the framework of mathematical programming with equilibrium constraints. This reformulation led to an augmented biconvex optimization problem with a bilinear equality constraint, which was effectively solved by

a penalty method. In a broader context, [36] proposed a continuous $l_p$-norm (for $p > 0$) boxed reformulation and used the alternating direction method of multipliers to solve it.

### 1.2 Contribution

In this paper, we introduce a sharp-peak function (SPF) to derive the model (SPCO). Consequently, our approach serves as an equivalent reformulation, as shown in Table 1. Most importantly, the new model provides strong theoretical guarantees and enables the development of an efficient numerical algorithm. In other words, it offers a practical and effective continuous optimization approach for solving the discrete programming problem (UBIP). The main contributions are fourfold.

*1) The invention of SPFs.* We introduce SPFs to equivalently transform binary constraints into equality constraints. These functions are highly general, capable of accommodating a wide range of fundamental functions. Importantly, when the penalty method is applied to solve problem (SPCO), SPFs facilitate the development of a new exact penalty theorem, a result that other existing functions, such as the piecewise function [40], $\ell_2$ norm[22, 26], and $\ell_p$ norm with $p > 1$ [36], may fail to achieve. A counterexample is given in (3.5) to illustrate this.

*2) New exact penalty theorems.* To address (SPCO), an equivalent model of (UBIP), we investigate its penalty model by showing that the global minimizers to (SPCO) and the penalty model coincide when the penalty parameter exceeds a threshold, a constant that is independent of the solution set of (SPCO). This contrasts with traditional exact penalty theory, where the penalty parameter typically depends on the solution set of the original problem. Furthermore, we introduce the concepts of Karush-Kuhn-Tucker (KKT) points and P-stationary points of the penalty model, which allow for a more comprehensive optimality analysis by revealing their relationships with local and global minimizers for (SPCO), as illustrated in Figure 3. These relationships suggest that targeting a P-stationary point for the penalty problem is a promising way to solve (UBIP), leading to an effective algorithm based on the scheme of the P-stationary point.

*3) A simple algorithm with convergence guarantees.* To solve the penalized problem, we propose an algorithm named ShaPeak, built upon the inexact alternating direction method of multipliers (iADMM) with an adaptively updated penalty parameter. The inexactness in solving subproblems and the adaptive penalty update pose challenges for convergence analysis. Nevertheless, we establish that the whole sequence converges to a P-stationary point in a linear rate, provided that parameters are chosen properly and $\nabla f$ is locally Lipschitz continuous on a bounded box.

*4) Superior numerical performance.* We benchmark ShaPeak against several state-of-the-art solvers, including the commercial solver GUROBI, which is designed for quadratic and linear problems. In addition to these problems, ShaPeak is also capable of handling non-quadratic applications effectively. The numerical experiments demonstrate that ShaPeak achieves superior accuracy and computational efficiency.

### 1.3 Organization

The paper is organized as follows. In the next subsection, we introduce the notation and functions used throughout the paper. Section 2 defines SPFs and presents two special examples. Section 3

presents the penalty model for (SPCO) and establishes the exact penalty theory. In Section 4, we develop the algorithm and analyze its convergence properties. The final two sections are dedicated to extensive numerical experiments and concluding remarks.

### 1.4 Preliminaries

The 1-dimensional and $n$-dimensional unit boxes are denoted by

$$B := \{x \in \mathbb{R} : 0 \leqslant x \leqslant 1\}, \qquad \mathbb{B} := \{\mathbf{x} \in \mathbb{R}^n : x_i \in B\}.$$

where ':=' means 'define'. For vector $\mathbf{x} \in \mathbb{R}^n$, we use $\|\mathbf{x}\|$ and $\|\mathbf{x}\|_\infty$ to denote its Euclidean and infinity norms. The indicator function of a given set $\Omega$ is defined by $\delta_\Omega(\mathbf{x}) = 0$ if $\mathbf{x} \in \Omega$ and $\delta_\Omega(\mathbf{x}) = \infty$ otherwise. Let $N_{\mathbb{B}}(\mathbf{x})$ be the normal cone [27] of $\mathbb{B}$ at $\mathbf{x}$. Then any $\mathbf{v} \in N_{\mathbb{B}}(\mathbf{x})$ satisfies

$$v_i \in \begin{cases} (-\infty, 0], & \text{if } x_i = 0, \\ \{0\}, & \text{if } x_i \in (0,1), \\ [0, +\infty), & \text{if } x_i = 1. \end{cases} \tag{1.1}$$

For a lower semi-continuous function $f : \mathbb{R}^n \to \mathbb{R}$, the definition of the (limiting) subdifferential denoted by $\partial f$ can be found in [27, Definition 8.3]. The proximal operator of a function $\varphi : \mathbb{R}^n \to \mathbb{R}$, associated with a parameter $\tau > 0$, is defined by

$$\mathrm{Prox}_{\tau\varphi}(\mathbf{z}) := \underset{\mathbf{x}\in\mathbb{R}^n}{\mathrm{argmin}} \ \varphi(\mathbf{x}) + \frac{1}{2\tau}\|\mathbf{x} - \mathbf{z}\|^2. \tag{1.2}$$

In particular, we write

$$\mathrm{Prox}^{\mathbb{B}}_{\tau\varphi}(\mathbf{z}) := \mathrm{Prox}_{\tau\varphi+\delta_{\mathbb{B}}}(\mathbf{z}). \tag{1.3}$$

We say function $f$ is $L$-strong smoothness on $\Omega \subseteq \mathbb{R}^n$ if

$$f(\mathbf{x}) \leqslant f(\mathbf{w}) + \langle \nabla f(\mathbf{w}), \mathbf{x} - \mathbf{w}\rangle + \frac{L}{2}\|\mathbf{x} - \mathbf{w}\|^2, \quad \forall\, \mathbf{x}, \mathbf{w} \in \Omega,$$

where $L > 0$. We say function $h : \Omega \to \mathbb{R}^m$ is locally Lipschitz continuous at point $\mathbf{x} \in \Omega$ if

$$\|h(\mathbf{w}) - h(\mathbf{v})\| \leqslant L(\mathbf{x})\|\mathbf{w} - \mathbf{v}\|$$

holds for any $\mathbf{w}$ and $\mathbf{v}$ around $\mathbf{x}$, where $L(\mathbf{x}) > 0$ is the Lipschitz constant relying on $\mathbf{x}$. Then function $h$ is said to be locally Lipschitz continuous on $\Omega$ if it is locally Lipschitz continuous at every point in $\Omega$. By Heine-Borel theorem, one can show that if function $h$ is locally Lipschitz continuous on a compact set $\Omega$, then $h$ is Lipschitz continuous on $\Omega$. Moreover, if $\nabla f$ is Lipschitz continuous on $\Omega \subseteq \mathbb{R}^n$ with a constant $L > 0$, then $f$ is $L$-strong smooth on $\Omega \subseteq \mathbb{R}^n$. A function $f$ is said to be $\ell$-strong convex on $\Omega \subseteq \mathbb{R}^n$ if

$$f(\mathbf{x}) \geqslant f(\mathbf{w}) + \langle \nabla f(\mathbf{w}), \mathbf{x} - \mathbf{w}\rangle + \frac{\ell}{2}\|\mathbf{x} - \mathbf{w}\|^2, \quad \forall\, \mathbf{x}, \mathbf{w} \in \Omega,$$

where $\ell > 0$. Finally, we define a useful operator by

$$\Pi(r, s, u, v) = \begin{cases} \{r\}, & u < v, \\ \{r, s\}, & u = v, \\ \{s\}, & u > v. \end{cases} \tag{1.4}$$

## 2 Sharp-Peak Functions

We now introduce the sharp-peak function (SPF) that can be employed to equivalently reformulate the binary constraint as an equality constraint.

**Definition 2.1** (Sharp-Peak Functions)**.** *Function $g : \mathbb{R} \to \mathbb{R} \cup \{\infty\}$ is called a sharp-peak function if it satisfies the following conditions:*

*c1) For any $x \in B$, $g(x) \geqslant 0$ and $g(x) = 0$ if and only if $x \in \{0, 1\}$.*

*c2) $g$ is lower semi-continuous on $B$ and there exists a $c > 0$ such that*

$$|\nu| \geqslant c, \quad \forall\ \nu \in \partial g(x),\ \forall\ x \in B. \tag{2.1}$$

*c3) $\partial(g(x) + \delta_B(x)) = \partial g(x) + N_B(x)$ for any $x \in \{0, 1\}$.*

According to c1) and c2), function $g$ has a sharp peak within interval $(0, 1)$, see functions in Figures 1 and 2. Therefore, we call it the sharp-peak function. In (2.1), there is a uniform positive lower bound $c$. This is not a strict condition. In fact, if $c_0 := \inf\{|\nu| : x \in B, \nu \in \partial g(x)\} > 0$, then $c$ can be set as $c = c_0$. For example, $g(x) = 1 - |2x - 1|$ and $c = 2$. Some sufficient conditions to ensure c3) include $g(x)$ being continuously differentiable or being regular at $x = 0$ and $x = 1$. A class of SPFs can be given as follows,

$$g(x) = \psi(1 - |2x - 1|^p), \quad p \in (0, 1], \tag{2.2}$$

where $\psi$ satisfies that i) $\psi(0) = 0$, ii) $\psi$ is continuous differentiable on $B$, and iii) $\inf_{t\in B} \psi'(t) > 0$. Therefore, $\psi$ can be various basic functions, such as, $|t|^q$ with $q \in (0, 1]$, $|t + 1|^r - 1$ with $r \geq 1$, $\log(1+t)$, $e^t - 1$, $\sin(t)$, and $\tan(t)$; see their plots in Figure 1. We point out that $g(x) = 1 - |2x - 1|^p$ with $p \in (0, 1]$ corresponding to $g$ in (2.2) with $\psi(t) = t$ has been studied in [36]. However, $g(x) = 1 - |2x - 1|^p$ with $p > 1$ in [36] and $g(x) = x(1 - x)$ in [40] are not SPFs due to $g'(1/2) = 0$.

In what follows, we introduce two useful SPFs that cover a broad class of basic functions and facilitate the design of an efficient numerical algorithm.

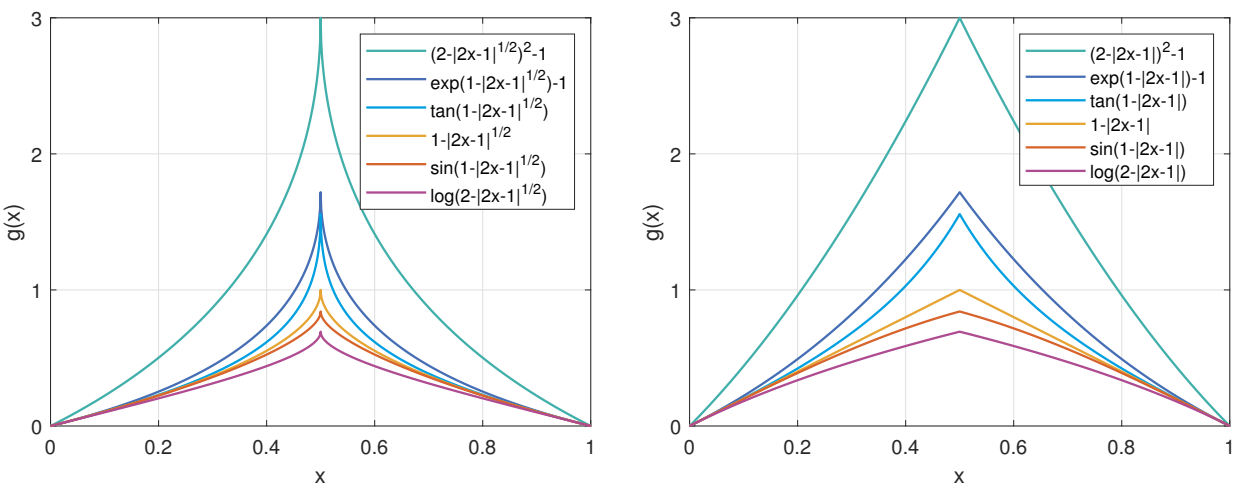


Figure 1: Plots of $\psi(1 - |2x - 1|^p)$.

**Lemma 2.1.** *Given $a \geqslant 1, b \geqslant 1, p > 0, q > 0$, and $\omega \in [0,1]$, let $g$ be defined by*

$$g(x;\omega,a,b,p,q) = \begin{cases} \dfrac{|x+a|^p}{p} - \dfrac{a^p}{p} \quad =: g_1(x,a,p), & x < \omega, \\ \min\Big\{g_1(\omega,a,p),\ g_2(\omega,b,q)\Big\}, & x = \omega, \\ \dfrac{|x-1-b|^q}{q} - \dfrac{b^q}{q} \quad =: g_2(x,b,q), & x > \omega, \end{cases} \tag{2.3}$$

*and $h$ be defined by*

$$h(x;\omega,a,b,p,q) = \begin{cases} \dfrac{a^p}{p} - \dfrac{|x-a|^p}{p} \quad =: h_1(x,a,p), & x < \omega, \\ \min\Big\{h_1(\omega,a,p),\ h_2(\omega,b,q)\Big\}, & x = \omega, \\ \dfrac{b^q}{q} - \dfrac{|x-1+b|^q}{q} \quad =: h_2(x,b,q), & x > \omega. \end{cases} \tag{2.4}$$

*Then both functions are SPFs.*

*Proof.* We prove the results for the function $g$ only, as the proof for the function $h$ follows similarly. It is easy to check that both functions are lower semi-continuous on $B$ and satisfy c1) in Definition c1). The remaining parts of c2) and c3) are proved in three cases.

Case 1: $\omega \in (0,1)$. Under such a case, we have

- when $x \in [0,\omega)$, $\partial g(x;\omega,a,b,p,q) = \{(x+a)^{p-1}\}$;
- when $x \in (\omega,1]$, $\partial g(x;\omega,a,b,p,q) = \{-(b+1-x)^{q-1}\}$;
- when $x = \omega$, by letting

$$g_1 := \frac{|\omega+a|^p}{p} - \frac{a^p}{p}, \qquad g_2 := \frac{|\omega-1-b|^q}{q} - \frac{b^q}{q},$$

  one can check that

$$\partial g(x;\omega,a,b,p,q) = \begin{cases} [(\omega+a)^{p-1},\infty), & g_1 < g_2, \\ \{(\omega+a)^{p-1}, -(b+1-\omega)^{q-1}\}, & g_1 = g_2, \\ (-\infty, -(b+1-\omega)^{q-1}], & g_1 > g_2. \end{cases} \tag{2.5}$$

Therefore, for any $\nu \in \partial g(x;\omega,a,b,p,q)$ and any $t \in (0,1)$, it follows

$$|\nu| \geqslant \min\left\{(\omega+a)^{p-1}, a^{p-1}, (b+1-\omega)^{q-1}, b^{q-1}\right\},$$

showing c2). We now verify c3) by the following two cases: If $x = 0$, then

$$\begin{aligned} \partial\left(g(0;\omega,a,b,p,q) + \delta_B(0)\right) &= (-\infty, a^{p-1}] = a^{p-1} + (-\infty, 0] \\ &= \partial g(0;\omega,a,b,p,q) + N_B(0). \end{aligned}$$

If $x = 1$, then

$$\begin{aligned} \partial\left(g(1;\omega,a,b,p,q) + \delta_B(1)\right) &= [b^{q-1},\infty) = b^{q-1} + [0,\infty) \\ &= \partial g(1;\omega,a,b,p,q) + N_B(1). \end{aligned} \tag{2.6}$$

Case 2: $\omega = 0$. Under such a case, it holds

$$g(x;0,a,b,p,q) = \begin{cases} 0, & x = 0 \\ \dfrac{|x-1-b|^q}{q} - \dfrac{b^q}{q}, & x \in (0,1], \end{cases}$$

$$\partial g(x;0,a,b,p,q) = \begin{cases} [a^{p-1}, \infty), & x = 0 \\ \{-(b+1-x)^{q-1}\}, & x \in (0,1]. \end{cases}$$

Therefore, for any $\nu \in \partial g(x;0,a,b,p,q)$ and any $x \in (0,1)$, the above condition results in

$$|\nu| \geqslant \min\left\{a^{p-1}, (b+1)^{q-1}, b^{q-1}\right\}.$$

Moreover, one can check that (2.6) holds for $x = 1$. For $x = 0$,

$$\begin{aligned} \partial\left(g(0;0,a,b,p,q) + \delta_B(0)\right) &= (-\infty, \infty) = [a^{p-1}, \infty) + (-\infty, 0] \\ &= \partial g(0;0,a,b,p,q) + N_B(0). \end{aligned}$$

Hence, c2) and c3) are satisfied.

Case 3: $\omega = 1$. The proof follows similarly to the case where $\omega = 0$. □

Examples of $g(x;\omega,a,b,p,q)$ and $h(x;\omega,a,b,p,q)$ can be found in Figure 2. When $a = b$, $p = q$, and $\omega \in (0,1)$, both functions are continuous on $B$. For most cases, they are discontinuous at $t = u$. Note that for when $\omega = 1$ or $\omega = 0$, functions $g$ and $h$ on $B$ can be expressed as

$$g(x;0,a,b,p,q) = \frac{|x-(x)_{0/1}-b|^q}{q} - \frac{b^q}{q}, \qquad g(x;1,a,b,p,q) = \frac{|x(1-x)_{0/1}+a|^p}{p} - \frac{a^p}{p},$$

$$h(x;0,a,b,p,q) = \frac{b^q}{q} - \frac{|x-(x)_{0/1}+b|^q}{q}, \qquad h(x;1,a,b,p,q) = \frac{a^p}{p} - \frac{|x(1-x)_{0/1}-a|^p}{p},$$

where $(x)_{0/1}$ is the so-called step function or 0/1 loss function [31, 41] defined by

$$(x)_{0/1} = \begin{cases} 1, & x > 0, \\ 0, & x \leqslant 0. \end{cases}$$

To end this section, we derive the proximal operators of $g(x;\omega,a,b,p,q)$ and $h(x;\omega,a,b,p,q)$.

**Lemma 2.2.** *Let $g(x;\omega,a,b,p,q)$ and $h(x;\omega,a,b,p,q)$ be defined by (2.3), and*

$$\begin{aligned} x_1^* &= \operatorname{argmin}_{x\in[0,\omega]}\ \phi_1(x) := \frac{(x-z)^2}{2\tau} + \frac{(x+a)^p}{p} - \frac{a^p}{p}, \\ x_2^* &= \operatorname{argmin}_{x\in[\omega,1]}\ \phi_2(x) := \frac{(x-z)^2}{2\tau} + \frac{(1+b-x)^q}{q} - \frac{b^q}{q}, \\ x_3^* &= \operatorname{argmin}_{x\in[0,\omega]}\ \phi_3(x) := \frac{(x-z)^2}{2\tau} - \frac{(a-x)^p}{p} + \frac{a^p}{p}, \\ x_4^* &= \operatorname{argmin}_{x\in[\omega,1]}\ \phi_4(x) := \frac{(x-z)^2}{2\tau} - \frac{(x-1+b)^q}{q} + \frac{b^q}{q}. \end{aligned} \tag{2.7}$$

*Then two proximal operators are computed by*

$$\operatorname{Prox}^B_{\tau g(\cdot;\omega,a,b,p,q)}(z) = \Pi\left(x_1^*, x_2^*, \phi_1(x_1^*), \phi_2(x_2^*)\right),$$

$$\operatorname{Prox}^B_{\tau h(\cdot;\omega,a,b,p,q)}(z) = \Pi\left(x_3^*, x_4^*, \phi_3(x_3^*), \phi_4(x_4^*)\right).$$

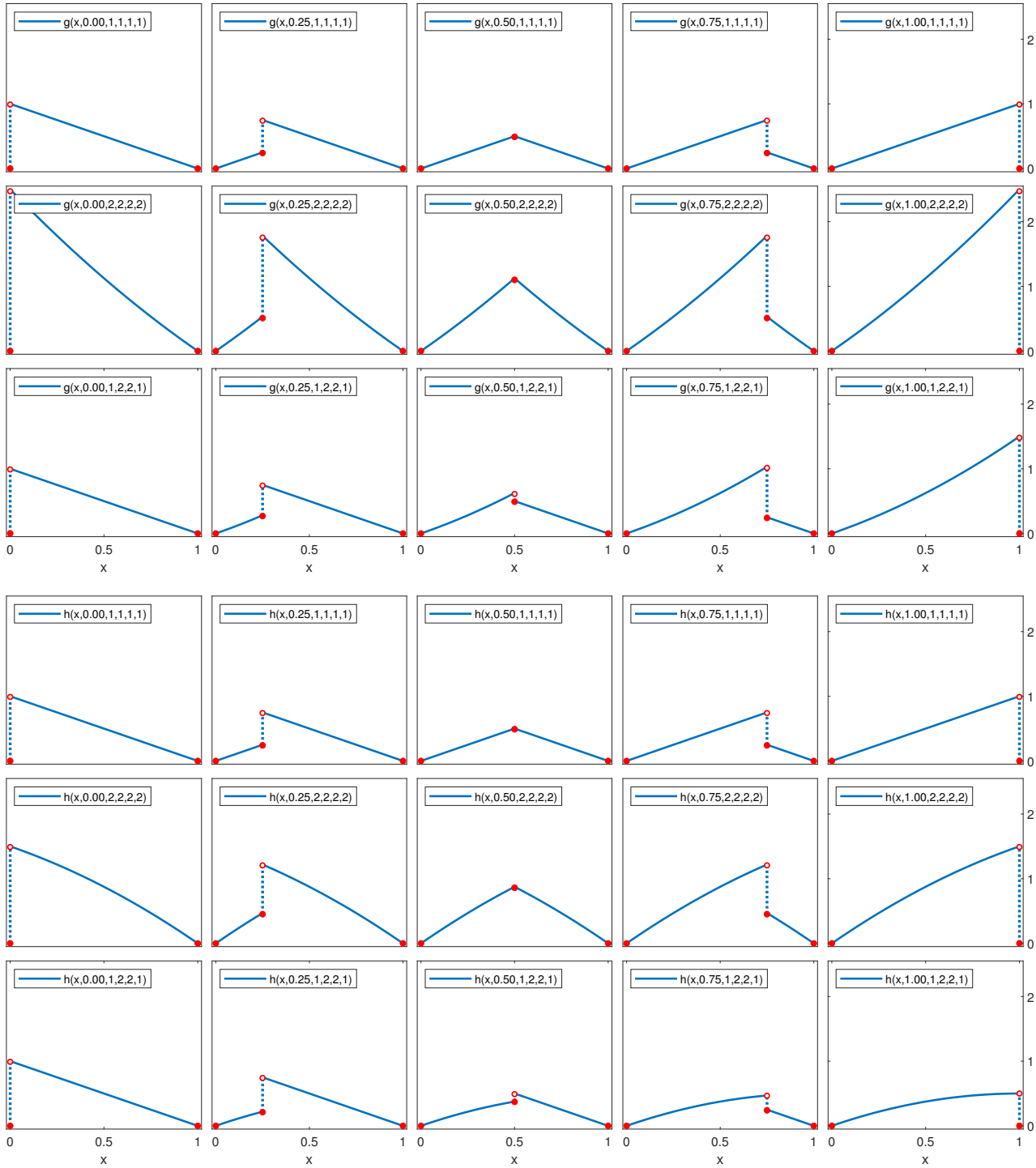


Figure 2: Examples of $g(x;\omega,a,b,p,q)$ and $h(x;\omega,a,b,p,q)$.

*Proof.* By decomposing $B=[0,\omega]\cup[\omega,1]$, one can just compare $\phi_1(x_1^*)$ and $\phi_2(x_2^*)$ (resp. $\phi_3(x_3^*)$ and $\phi_4(x_4^*)$) to derive $\mathrm{Prox}_{\tau g}^{B}$ (resp. $\mathrm{Prox}_{\tau h}^{B}$). □

One can observer that $x_1^*, x_2^*, x_3^*$, and $x_4^*$ admit closed-form solutions when $p,q\in\{1/2,2/3,1,2\}$, leading to explicit expressions for the two proximal operators. Table 2 lists several closed-form solutions for case $p,q\in\{1,2\}$, where $\kappa_1 := \sqrt{(\tau+\tau^2)(2a+1)}-\tau-a\tau$ and $\kappa_2 := \sqrt{(\tau-\tau^2)(2a-1)}+\tau-a\tau$. Moreover, when $\tau$ exceeds a certain threshold, the proximal operators of $g$ and $h$ yield only binary elements, highlighting the effectiveness of SPFs in binary integer programming.

Table 2: Closed forms of proximal operators $\mathrm{Prox}^{B}_{\tau g(\cdot,\omega,a,b,p,q)}(z)$ and $\mathrm{Prox}^{B}_{\tau h(\cdot,\omega,a,b,p,q)}(z)$.

| $(\omega, a, b, p, q)$ | $\tau \geq 1/2$ | $0 < \tau \leqslant 1/2$ |
|---|---|---|
| $g(\cdot, 0, 1, 1, 1, 1)$ | $\begin{cases} 0, & z < 1/2 \\ \{0, 1\}, & z = 1/2 \\ 1, & z > 1/2 \end{cases}$ | $\begin{cases} 0, & z < \sqrt{2\tau} - \tau \\ \{0, z + \tau\}, & z = \sqrt{2\tau} - \tau \\ z + \tau, & z \in (\sqrt{2\tau} - \tau, 1 - \tau) \\ 1, & z \geqslant 1 - \tau \end{cases}$ |
| $g(\cdot, 1, 1, 1, 1, 1)$ | $\begin{cases} 0, & z < 1/2 \\ \{0, 1\}, & z = 1/2 \\ 1, & z > 1/2 \end{cases}$ | $\begin{cases} 0, & z \leqslant \tau \\ z - \tau, & z \in (\tau, 1 + \tau - \sqrt{2\tau}) \\ \{1, z - \tau\}, & z = 1 + \tau - \sqrt{2\tau} \\ 1, & z > 1 + \tau - \sqrt{2\tau} \end{cases}$ |
| $g(\cdot, 1/2, 1, 1, 1, 1)$ | $\begin{cases} 0, & z < 1/2 \\ \{0, 1\}, & z = 1/2 \\ 1, & z > 1/2 \end{cases}$ | $\begin{cases} 0, & z \leqslant \tau \\ z - \tau, & z \in (\tau, 1/2) \\ \{z - \tau, z + \tau\}, & z = 1/2 \\ z + \tau, & z = (1/2, 1 - \tau) \\ 1, & z \geqslant 1 - \tau \end{cases}$ |
| | $\tau \geq 1/(2a)$ | $0 < \tau \leqslant 1/(2a)$ |
| $g(\cdot, 0, a, a, 2, 2)$ | $\begin{cases} 0, & z < 1/2 \\ \{0, 1\}, & z = 1/2 \\ 1, & z > 1/2 \end{cases}$ | $\begin{cases} 0, & z < \kappa_1 \\ \{0, \frac{z+(1+a)\tau}{1+\tau}\}, & z = \kappa_1 \\ \frac{z+(1+a)\tau}{1+\tau}, & z \in (\kappa_1, 1 - a\tau) \\ 1, & z \geqslant 1 - a\tau \end{cases}$ |
| $g(\cdot, 1, a, a, 2, 2)$ | $\begin{cases} 0, & z < 1/2 \\ \{0, 1\}, & z = 1/2 \\ 1, & z > 1/2 \end{cases}$ | $\begin{cases} 0, & z \leqslant a\tau \\ \frac{z-a\tau}{1+\tau}, & z \in (a\tau, 1 - \kappa_1) \\ \{\frac{z-a\tau}{1+\tau}, 1\}, & z = 1 - \kappa_1 \\ 1, & z > 1 - \kappa_1 \end{cases}$ |
| $g(\cdot, 1/2, a, a, 2, 2)$ | $\begin{cases} 0, & z < 1/2 \\ \{0, 1\}, & z = 1/2 \\ 1, & z > 1/2 \end{cases}$ | $\begin{cases} 0, & z \leqslant a\tau \\ \frac{z-a\tau}{1+\tau}, & z \in (a\tau, 1/2) \\ \{\frac{z-a\tau}{1+\tau}, \frac{z+(1+a)\tau}{1+\tau}\}, & z = 1/2 \\ \frac{z+(1+a)\tau}{1+\tau}, & z = (1/2, 1 - a\tau) \\ 1, & z \geqslant 1 - a\tau \end{cases}$ |
| $h(\cdot, 0, a, a, 2, 2)$ | $\begin{cases} 0, & z < 1/2 \\ \{0, 1\}, & z = 1/2 \\ 1, & z > 1/2 \end{cases}$ | $\begin{cases} 0, & z < \kappa_2 \\ \{0, \frac{z+(a-1)\tau}{1-\tau}\}, & z = \kappa_2 \\ \frac{z+(a-1)\tau}{1-\tau}, & z \in (\kappa_2, 1 - a\tau) \\ 1, & z \geqslant 1 - a\tau \end{cases}$ |
| $h(\cdot, 1, a, a, 2, 2)$ | $\begin{cases} 0, & z < 1/2 \\ \{0, 1\}, & z = 1/2 \\ 1, & z > 1/2 \end{cases}$ | $\begin{cases} 0, & z \leqslant a\tau \\ \frac{z-a\tau}{1-\tau}, & z \in (a\tau, 1 - \kappa_2) \\ \{\frac{z-a\tau}{1-\tau}, 1\}, & z = 1 - \kappa_2 \\ 1, & z > 1 - \kappa_2 \end{cases}$ |
| $h(\cdot, 1/2, a, a, 2, 2)$ | $\begin{cases} 0, & z < 1/2 \\ \{0, 1\}, & z = 1/2 \\ 1, & z > 1/2 \end{cases}$ | $\begin{cases} 0, & z \leqslant a\tau \\ \frac{z-a\tau}{1-\tau}, & z \in (a\tau, 1/2) \\ \{\frac{z-a\tau}{1-\tau}, \frac{z+(a-1)\tau}{1-\tau}\}, & z = 1/2 \\ \frac{z+(a-1)\tau}{1-\tau}, & z = (1/2, 1 - a\tau) \\ 1, & z \geqslant 1 - a\tau \end{cases}$ |

## 3 Exact Penalty Theory

Instead of solving problem (SPCO), we aim to address its penalty model,

$$\min_{\mathbf{x}\in\mathbb{B}} \; F(\mathbf{x};\mu) := f(\mathbf{x}) + \mu\varphi(\mathbf{x}), \qquad \text{with} \;\; \mu > \overline{\mu} \;\; \text{and} \;\; \varphi(\mathbf{x}) := \sum_{i=1}^{n} g(x_i), \tag{EPM}$$

where $\overline{\mu}$ is defined by

$$\overline{\mu} := \max_{\mathbf{x}\in\mathbb{B}} \frac{\|\nabla f(\mathbf{x})\|_\infty}{c}. \tag{3.1}$$

Here, $c$ is relied on $g$ and defined in (2.1). Since $f$ is continuously differentiable, $\nabla f$ is continuous, which by the boundedness of $\mathbb{B}$ leads to the boundedness of $\overline{\mu}$. In the sequel, we show that problem (EPM) is indeed an exact penalty model of problem (SPCO).

### 3.1 KKT points

**Definition 3.1.** *Point $\widetilde{\mathbf{x}} \in \mathbb{B}$ is called a KKT point of problem (EPM) if it satisfies*

$$0 \in \nabla f(\widetilde{\mathbf{x}}) + \mu\partial\varphi(\widetilde{\mathbf{x}}) + N_{\mathbb{B}}(\widetilde{\mathbf{x}}). \tag{3.2}$$

Recalling (1.1), $\widetilde{\mathbf{x}} \in \mathbb{B}$ is a KKT point of (EPM) if and only if there is $\boldsymbol{\nu} \in \partial\varphi(\widetilde{\mathbf{x}})$ satisfying

$$\nabla_i f(\widetilde{\mathbf{x}}) + \mu\nu_i \begin{cases} \geqslant 0, & \text{if } \widetilde{x}_i = 0, \\ = 0, & \text{if } \widetilde{x}_i \in (0,1), \\ \leqslant 0, & \text{if } \widetilde{x}_i = 1. \end{cases} \tag{3.3}$$

Our first result establishes the first-order optimality condition for problem (EPM).

**Theorem 3.1.** *The following statements hold for problem (EPM).*

*1) Any KKT point is binary.*

*2) A KKT point is a local minimizer if $f$ and $\varphi$ are locally convex around this point.*

*3) A local minimizer is also a KKT point.*

*Proof.* 1) Suppose a KKT point $\widetilde{\mathbf{x}} \notin \{0,1\}^n$, namely, there is an $\widetilde{x}_i \in (0,1)$. Then there is $\nu_i \in \partial g(\widetilde{x}_i)$ such that $\nabla_i f(\widetilde{\mathbf{x}}) = -\mu\nu_i$ from (3.3), which by $|\nu_i| \geqslant c$ leads to the following contradiction,

$$c\overline{\mu} = \max_{\mathbf{x}\in\mathbb{B}} \|\nabla f(\mathbf{x})\|_\infty \geqslant |\nabla f(\widetilde{\mathbf{x}})| = \mu|\nu_i| \geqslant c\mu > c\overline{\mu}.$$

2) Let $\widetilde{\mathbf{x}}$ be a KKT point. Then $\widetilde{\mathbf{x}} \in \{0,1\}^n$ from 1). For any $\mathbf{x} \in \mathbb{B}$ around $\widetilde{\mathbf{x}}$, the local convexity of $f$ and $\varphi$ enables that

$$F(\widetilde{\mathbf{x}};\mu) - F(\mathbf{x};\mu) \geqslant \langle \nabla f(\widetilde{\mathbf{x}}) + \mu\boldsymbol{\nu}, \widetilde{\mathbf{x}} - \mathbf{x}\rangle \geqslant 0,$$

where $\boldsymbol{\nu} \in \varphi(\widetilde{\mathbf{x}})$ and the last inequality is from (3.2).

3) By Definition 2.1 c3), for any $x \in \{0,1\}$, we have

$$\partial(g(x) + \delta_B(x)) = \partial g(x) + N_B(x).$$

For any $x \in (0,1)$, there is $\delta_B(x) = 0$ and $N_B(x) = \emptyset$. This means the above condition holds for any $x \in B$, thereby resulting in

$$\partial(\mu\varphi(\widetilde{\mathbf{x}}) + \delta_{\mathbb{B}}(\widetilde{\mathbf{x}})) = \mu\partial\varphi(\widetilde{\mathbf{x}}) + N_{\mathbb{B}}(\widetilde{\mathbf{x}}).$$

By Fermat's rule [27, Theorem 10.1(P422)], if $\widetilde{\mathbf{x}}$ is a local minimizer of (EPM), then

$$\begin{aligned} 0 &\in \partial(f(\widetilde{\mathbf{x}}) + \mu\varphi(\widetilde{\mathbf{x}}) + \delta_{\mathbb{B}}(\widetilde{\mathbf{x}})) \\ &= \nabla f(\widetilde{\mathbf{x}}) + \partial(\mu\varphi(\widetilde{\mathbf{x}}) + \delta_{\mathbb{B}}(\widetilde{\mathbf{x}})) \\ &= \nabla f(\widetilde{\mathbf{x}}) + \mu\partial\varphi(\widetilde{\mathbf{x}}) + N_{\mathbb{B}}(\widetilde{\mathbf{x}}), \end{aligned} \tag{3.4}$$

where the first equation is from three facts: 1) $f$ is continuously differentiable, 2) $\varphi(\widetilde{\mathbf{x}})$ is lower semi-continuous and bounded, and 3) [27, 10.10 Exercise]. □

In the above theorem, the assumption of the local convexity of $\varphi$ around a KKT point is mild. In fact, many SPFs $g(z)$ are locally convex at $z = 0$ and $z = 1$. Examples include $g(x) = 1 - |2x - 1|$, as well as function $g(x; \omega, a, b, p, q)$ with any $\omega \in (0,1)$ and $p = 1$ or 2 defined in (2.3). This means $\varphi(\mathbf{x}) = \sum_{i=1}^n g(x_i)$ is locally convex at any $\mathbf{x} \in \mathbb{B}$. Together with the binary nature of KKT points, this local convexity condition suffices to meet the assumption in the theorem. Now, we provide an example to illustrate Theorem 3.1 as well as the advantage of using SPFs over some existing functions, such as $g(x) = x(1-x)$ studied in [40].

**Example 3.1.** *Given $s \in (1,2)$, consider the following two problems,*

$$\min_{x \in B} \; F(x;\mu) = (1/s)\,|x - 1/2|^s + \mu x(1-x), \tag{3.5}$$

$$\min_{x \in B} \; F(x;\mu) = (1/s)\,|x - 1/2|^s + \mu g(x; 1/2, 1, 1, 2, 2). \tag{3.6}$$

- *Problem (3.5) always has a local minimizer $1/2$ for any given $\mu > 0$. In fact, $\partial F(1/2;\mu) = \{0\}$ for any given $\mu$. Moreover, for any sufficiently small $|\varepsilon|$, we have*

$$F(1/2 + \varepsilon; \mu) - F(1/2; \mu) = |\varepsilon|^s / s + \mu\left(1/4 + \varepsilon^2\right) - \mu/4 = \left(|\varepsilon|^{p-1}/s - \mu\right)\varepsilon^2 \geqslant 0.$$

  *Therefore, $x = 1/2$ is a local minimizer of problem (3.5).*

- *Problem (3.6) always has binary local minimizers when $\mu > \overline{\mu} = 2^{1-s}$. In fact,*

$$0 \notin \partial F(x;\mu) = |x - 1/2|^{s-1} + \mu \begin{cases} \{x+1\}, & x \in (0, 1/2), \\ \{-3/2, 3/2\}, & x = 1/2, \\ \{x-2\}, & x \in (1/2, 1). \end{cases}$$

  *Therefore, the local minimizer of problem (3.6) can not lie within $(0,1)$. Two local (also global) minimizers are $x = 0$ and $x = 1$.*

This example illustrates that problem (EPM) with a penalty like $g(x) = x(1-x)$ may have non-binary local minimizers. In contrast, all local minimizers of the problem with SPFs are binary when $\mu$ is over a certain threshold. Based on Theorem 3.1, we establish the exact penalty theorem for problems (SPCO) and (EPM).

**Theorem 3.2** (Exact Penalty Theorem)**.** *A point is a global minimizer of problem (SPCO) if and only if it is a global minimizer of problem (EPM).*

*Proof.* Let $\mathbf{x}^*$ and $\widetilde{\mathbf{x}}$ be global minimizers of problems (SPCO) and (EPM), respectively. Then, $\widetilde{\mathbf{x}}$ is a KKT point of problem (EPM) and thus $\widetilde{\mathbf{x}} \in \mathcal{F} := \{0,1\}^n$ by Theorem 3.1. Since the feasible region of (SPCO) is $\mathcal{F}$, it follows $f(\mathbf{x}^*) \leqslant f(\widetilde{\mathbf{x}})$, leading to

$$F(\widetilde{\mathbf{x}};\mu) \leqslant F(\mathbf{x}^*;\mu) = f(\mathbf{x}^*) \leqslant f(\widetilde{\mathbf{x}}) = F(\widetilde{\mathbf{x}};\mu).$$

where the first inequality holds because of the optimality of $\widetilde{\mathbf{x}}$ to problem (EPM) and $\mathbf{x}^* \in \mathcal{F} \subseteq \mathbb{B}$, the two equations hold due to $\varphi(\mathbf{x}^*) = \varphi(\widetilde{\mathbf{x}}) = 0$. The above condition implies the four values are the same, concluding the conclusion. □

**Remark 3.1.** *Theorem 3.2 means that the global minimizers to problem (SPCO) (equivalent to problem (UBIP)) and its penalty model (EPM) coincide when $\mu > \overline{\mu}$, while threshold $\overline{\mu}$ defined in (3.1) is independent of the solution set of (SPCO). This contrasts with traditional exact penalty theory (e.g., [23, Theorem 17.3]), where the penalty parameter relies on the solution to the original problem. A similar result to Theorem 3.2 has been established in [39] if $f$ is Lipschitz continuous and convex on $\mathbb{B}$. However, no additional conditions on $f$ are imposed to derive Theorem 3.2.*

### 3.2 P-stationary point

In this subsection, to facilitate the algorithm development for solving problem (EPM), we define a P-stationary point associated with the proximal operator of $\varphi$.

**Definition 3.2.** *Point $\overline{\mathbf{x}}$ is called a P-stationary point of (EPM) if there is a $\tau > 0$ such that*

$$\overline{\mathbf{x}} \in \mathrm{Prox}^{\mathbb{B}}_{\tau\mu\varphi}\Big(\overline{\mathbf{x}} - \tau\nabla f(\overline{\mathbf{x}})\Big) = \mathrm{argmin}_{\mathbf{z}\in\mathbb{B}}\ \frac{1}{2}\|\mathbf{z} - (\overline{\mathbf{x}} - \tau\nabla f(\overline{\mathbf{x}}))\|^2 + \tau\mu\varphi(\mathbf{z}). \tag{3.7}$$

It is worth noting that many SPFs $g$ enable a closed-form of $\mathrm{Prox}^{\mathbb{B}}_{\tau\mu\varphi}$, see Lemma 2.2, thereby enabling the design of an efficient numerical algorithm presented in the next section. By applying similar reasoning to derive (3.4), we obtain the necessary optimality condition of (3.7) as follows,

$$\begin{aligned} 0 &\in \partial\left(\frac{1}{2}\|\overline{\mathbf{x}} - (\overline{\mathbf{x}} - \tau\nabla f(\overline{\mathbf{x}}))\|^2 + \tau\mu\varphi(\overline{\mathbf{x}}) + \delta_{\mathbb{B}}(\overline{\mathbf{x}})\right) \\ &= \tau\nabla f(\overline{\mathbf{x}}) + \tau\mu\partial\varphi(\overline{\mathbf{x}}) + N_{\mathbb{B}}(\overline{\mathbf{x}}), \end{aligned} \tag{3.8}$$

which suffices to condition (3.2), so a P-stationary point is a KKT point. The following result establishes the relationships among P-stationary points, KKT points, and local minimizers of (EPM).

**Theorem 3.3.** *The following relationships hold for problem (EPM).*

1) *A P-stationary point is a KKT point. Conversely, a KKT point is a P-stationary point if $\varphi$ is locally convex around this point.*

2) *A local minimizer is a P-stationary point if $f$ and $\varphi$ are locally convex around this point or $f$ is $L$-strongly smooth on $\mathbb{B}$.*

3) *A P-stationary point with $\tau \geqslant 1/\ell$ is a global minimizer if $f$ is $\ell$-strongly convex on $\mathbb{B}$.*

*Proof.* 1) It follows from (3.8) that a P-stationary point is a KKT point. Conversely, let $\widetilde{\mathbf{x}}$ be a KKT point of (EPM). Then $\widetilde{\mathbf{x}} \in \{0,1\}^n$ by Theorem 3.1. Let $\mathbf{z}$ satisfy

$$\mathbf{z} \in \mathrm{Prox}^{\mathbb{B}}_{\tau\mu\varphi}(\widetilde{\mathbf{x}} - \tau\nabla f(\widetilde{\mathbf{x}})). \tag{3.9}$$

By the definition of $\mathrm{Prox}^{\mathbb{B}}_{\tau\mu\varphi}$, we obtain

$$\|\mathbf{z} - (\widetilde{\mathbf{x}} - \tau\nabla f(\widetilde{\mathbf{x}}))\|^2 + 2\tau\mu\varphi(\mathbf{z}) \geqslant \|\widetilde{\mathbf{x}} - (\widetilde{\mathbf{x}} - \tau\nabla f(\widetilde{\mathbf{x}}))\|^2 + 2\tau\mu\varphi(\widetilde{\mathbf{x}}),$$

which by the local convexity of $\varphi$, (3.2), and $\mathbf{z} \in \mathbb{B}$ results in

$$\begin{aligned} -\|\mathbf{z} - \widetilde{\mathbf{x}}\|^2 &\geqslant 2\tau\langle \mathbf{z} - \widetilde{\mathbf{x}}, \nabla f(\mathbf{x})\rangle + 2\tau\mu(\varphi(\mathbf{z}) - \varphi(\widetilde{\mathbf{x}})) \\ &\geqslant 2\tau\langle \mathbf{z} - \widetilde{\mathbf{x}}, \nabla f(\widetilde{\mathbf{x}}) + \mu\boldsymbol{\nu}\rangle \geqslant 0, \end{aligned} \tag{3.10}$$

where $\boldsymbol{\nu} \in \partial\varphi(\widetilde{\mathbf{x}})$. The above condition delivers $\mathbf{z} = \widetilde{\mathbf{x}}$. Therefore, $\widetilde{\mathbf{x}}$ is a P-stationary point.

2) If $f$ and $\varphi$ are locally convex around this point, then from Theorem 3.1, a local minimizer is a KKT, which by 1) indicates that it is a P-stationary point. Now we consider the case of strong smoothness of $f$ on $\mathbb{B}$. Let $\mathbf{x}$ be a local minimizer of (EPM) and $\mathbf{z}$ satisfy $\mathbf{z} \in \mathrm{Prox}^{\mathbb{B}}_{\tau\mu\varphi}(\mathbf{x} - \tau\nabla f(\mathbf{x}))$. Then it is a KKT point and $\mathbf{x} \in \{0,1\}^n$ from Theorem 3.1, thereby $\varphi(\mathbf{x}) = 0$. Similar reasoning allows us to derive the first inequality in (3.10), namely,

$$\begin{aligned} \|\mathbf{z} - \mathbf{x}\|^2 &\leqslant 2\tau\langle \mathbf{x} - \mathbf{z}, \nabla f(\mathbf{x})\rangle + 2\tau\mu(\varphi(\mathbf{x}) - \varphi(\mathbf{z})) \\ &\leqslant 2\tau\|\mathbf{z} - \mathbf{x}\|\|\nabla f(\mathbf{x})\| \end{aligned}$$

where the second inequality is due to $\varphi(\mathbf{x}) = 0$ and $\varphi(\mathbf{z}) \geqslant 0$, which implies $\|\mathbf{z} - \mathbf{x}\| \leqslant 2\tau\|\nabla f(\mathbf{x})\|$ and thus $\mathbf{z}$ is around $\mathbf{x}$ when $\tau$ is sufficiently small. By the $L$-strong smoothness of $f$ on $\mathbb{B}$ and the first inequality in (3.10),

$$\begin{aligned} 2F(\mathbf{z};\mu) - 2F(\mathbf{x};\mu) &\leqslant 2\langle \mathbf{z} - \mathbf{x}, \nabla f(\mathbf{x})\rangle + 2\mu(\varphi(\mathbf{z}) - \varphi(\mathbf{x})) + L\|\mathbf{z} - \mathbf{x}\|^2 \\ &\leqslant (L - 1/\tau)\,\|\mathbf{z} - \mathbf{x}\|^2 \leqslant 0, \end{aligned}$$

where the last inequality is because $\tau$ is sufficiently small. The above condition leads to $\mathbf{z} = \mathbf{x}$ due to the local optimality of $\mathbf{x}$, namely, $\mathbf{x}$ is a P-stationary point.

3) Let $\overline{\mathbf{x}}$ be a P-stationary point. Then it satisfies

$$\overline{\mathbf{x}} \in \mathrm{Prox}^{\mathbb{B}}_{\tau\mu\varphi}(\overline{\mathbf{x}} - \tau\nabla f(\overline{\mathbf{x}})).$$

By the definition of $\mathrm{Prox}^{\mathbb{B}}_{\tau\mu\varphi}$, we obtain

$$\|\overline{\mathbf{x}} - (\overline{\mathbf{x}} - \tau\nabla f(\overline{\mathbf{x}}))\|^2 + 2\tau\mu\varphi(\overline{\mathbf{x}}) \leqslant \|\mathbf{w} - (\overline{\mathbf{x}} - \tau\nabla f(\overline{\mathbf{x}}))\|^2 + 2\tau\mu\varphi(\mathbf{w}),$$

for any $\mathbf{w} \in \mathbb{B}$, which results in

$$2\langle \overline{\mathbf{x}} - \mathbf{w}, \nabla f(\overline{\mathbf{x}})\rangle + 2\mu(\varphi(\overline{\mathbf{x}}) - \varphi(\mathbf{w})) \leqslant (1/\tau)\|\mathbf{w} - \overline{\mathbf{x}}\|^2. \tag{3.11}$$

Using the above condition and the $\ell$-strong convexity of $f$, we have

$$\begin{aligned} 2F(\overline{\mathbf{x}};\mu) - 2F(\mathbf{w};\mu) &\leqslant 2\langle \overline{\mathbf{x}} - \mathbf{w}, \nabla f(\overline{\mathbf{x}})\rangle + 2\mu(\varphi(\mathbf{x}) - \varphi(\mathbf{w})) - \ell\|\mathbf{w} - \overline{\mathbf{x}}\|^2 \\ &\leqslant (1/\tau - \ell)\,\|\mathbf{w} - \overline{\mathbf{x}}\|^2 \leqslant 0, \end{aligned}$$

due to $\tau \geqslant 1/\ell$. Therefore, $\overline{\mathbf{x}}$ is global minimizer of (EPM). □

Based on Theorems 3.1–3.3, we can establish the relationships among different solutions to problems (SPCO) and (EPM). These relationships suggest that pursuing a P-stationary point for problem (EPM) is a promising way to find a solution to (SPCO) or (UBIP).

**Corollary 3.1.** *The relationships among solutions to problems (UBIP), (SPCO), and (EPM) are given in Figure 3. For example, global minimizers of three problems coincide; a global minimizer of (EPM) is a P-stationary point if either $f$ and $\varphi$ are locally convex or $f$ is strongly smooth on $\mathbb{B}$; a P-stationary point of problem (EPM) is also a global minimizer if $f$ is strongly convex on $\mathbb{B}$.*

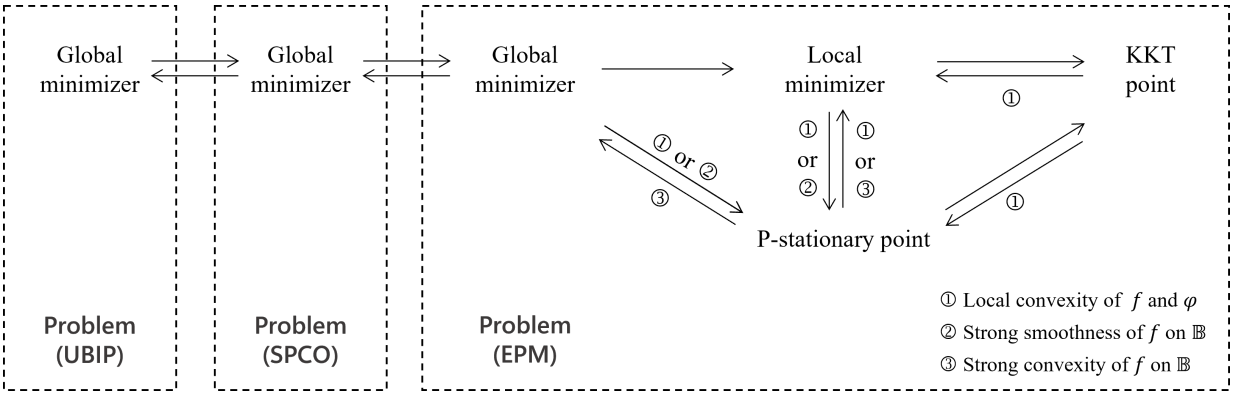


Figure 3: Relationship among different points for problems (UBIP) and (EPM).

**Example 3.2.** *Consider the following quadratic binary problem,*

$$\min_{\mathbf{x}\in\{0,1\}^2} \; f(\mathbf{x}) := (1/2)\,\langle \mathbf{x}, \mathbf{Q}\mathbf{x}\rangle + \langle \mathbf{q}, \mathbf{x}\rangle\,, \qquad \textit{with} \;\; \mathbf{Q} = \begin{bmatrix} 1 & -1 \\ -2 & 0 \end{bmatrix}, \;\; \mathbf{q} = \begin{bmatrix} -2 \\ 1/2 \end{bmatrix}. \tag{3.12}$$

*We aim to solve the following penalty model,*

$$\min_{\mathbf{x}\in\mathbb{B}} \; F(\mathbf{x};\mu) := (1/2)\,\langle \mathbf{x}, \mathbf{Q}\mathbf{x}\rangle + \langle \mathbf{q}, \mathbf{x}\rangle + \mu\varphi(\mathbf{x}), \tag{3.13}$$

*where $\varphi(\mathbf{x}) = g(x_1; 1/2, 1, 1, 1, 1) + g(x_2; 1/2, 1, 1, 1, 1)$ and*

$$g(x; 1/2, 1, 1, 1, 1) = \begin{cases} x, & \text{if } x \leqslant 1/2, \\ 1 - x, & \text{if } x \geqslant 1/2. \end{cases}$$

The objective is strongly smooth but is nonconvex since $\mathbf{Q}$ has two eigenvalues $-1$ and 2. One can verify that $c = 1$ and $\overline{\mu} = 3$. Therefore, according to Theorem 3.2, when $\mu > 3$, global minimizers to problems (3.12) and (3.13) coincide. The global minimizer is $\mathbf{x}^* = (1, 1)^\top$. Now, we verify the relationships between the global minimizer and a P-stationary point. By fixing $\mu = 4$ and $\tau = 1/2$, the following problem, one can check that

$$\mathrm{Prox}_{2\varphi}^{\mathbb{B}}\left(\mathbf{x} - \nabla f(\mathbf{x})/2\right) = \begin{cases} \{(1,0)^\top\}, & \text{if } \mathbf{x} = (0,0)^\top, \\ \{(1,1)^\top\}, & \text{if } \mathbf{x} = (1,0)^\top, (0,1)^\top, \text{ and } (1,1)^\top. \end{cases} \tag{3.14}$$

Therefore, $\mathbf{x}^*$ is the only point satisfying

$$\mathbf{x}^* \in \mathrm{Prox}_{2\varphi}^{\mathbb{B}}\left(\mathbf{x}^* - \nabla f(\mathbf{x}^*)/2\right),$$

namely, the only P-stationary point with $\tau = 1/2$ is $\mathbf{x}^*$. This justifies the relationship in Corollary 3.1 that a global minimizer of problem (EPM) is a P-stationary point if $f$ is strongly smooth on $\mathbb{B}$.

## 4 Algorithm and convergence

Rewrite problem (EPM) as

$$\min_{\mathbf{x},\mathbf{w}} \ f(\mathbf{x}) + \mu\varphi(\mathbf{w}), \quad \text{s.t. } \mathbf{x} - \mathbf{w} = \mathbf{0}, \ \mathbf{w} \in \mathbb{B}. \tag{4.1}$$

The corresponding augmented Lagrange function is

$$L(\mathbf{w}, \mathbf{x}, \mathbf{y}; \mu) = f(\mathbf{x}) + \mu\varphi(\mathbf{w}) + \langle \mathbf{y}, \mathbf{x} - \mathbf{w}\rangle + \frac{\sigma}{2}\|\mathbf{x} - \mathbf{w}\|^2, \tag{4.2}$$

where $\mathbf{y} \in \mathbb{R}^n$ is the Lagrange multiplier and $\sigma > 0$. We aim to solve problem (4.1) using a variant of the inexact alternating direction methods of multipliers (iADMM). Specifically, given current point $(\mathbf{w}^k, \mathbf{x}^k, \mathbf{y}^k; \mu_k)$, the next point is updated by

$$\mathbf{w}^{k+1} \in \operatorname{argmin}_{\mathbf{w}\in\mathbb{B}} \ \mu_k\varphi(\mathbf{w}) + \langle \mathbf{y}^k, \mathbf{x}^k - \mathbf{w}\rangle + \frac{\sigma}{2}\|\mathbf{x}^k - \mathbf{w}\|^2, \tag{4.3}$$

$$\mathbf{x}^{k+1} = \operatorname{argmin}_{\mathbf{x}} \ \langle \nabla f(\mathbf{w}^{k+1}) + \mathbf{y}^k, \mathbf{x} - \mathbf{w}^{k+1}\rangle + \frac{1}{2}\|\mathbf{x} - \mathbf{w}^{k+1}\|^2_{\mathbf{Q}^{k+1}} + \frac{\sigma}{2}\|\mathbf{x} - \mathbf{w}^{k+1}\|^2, \tag{4.4}$$

$$\mathbf{y}^{k+1} = \mathbf{y}^k + \sigma(\mathbf{x}^{k+1} - \mathbf{w}^{k+1}), \tag{4.5}$$

where $\mathbf{Q}^{k+1} \succeq \mathbf{0}$ is known as a pre-conditioning matrix updated adaptively during iterations or predefined in advance. Subproblem (4.3) is equivalent to

$$\mathbf{w}^{k+1} \in \operatorname{Prox}^{\mathbb{B}}_{(\mu_k/\sigma)\varphi}(\mathbf{x}^k + \mathbf{y}^k/\sigma). \tag{4.6}$$

Given particular $\varphi(\mathbf{x}) = \sum_{i=1}^n g(x_i)$, such as $g$ defined by (2.3) and (2.4), the above problem admits a closed-form solution due to Lemma 2.2. While for subproblem (4.4), we approximate $f(\mathbf{x})$ at $\mathbf{w}^{k+1}$ instead of $\mathbf{x}^k$ using a Taylor-like expansion. This design encourages $\mathbf{x}^{k+1}$ to approach $\mathbf{w}^{k+1}$ quickly, potentially leading to faster convergence. The solution to problem (4.4) is given by

$$\mathbf{x}^{k+1} = \mathbf{w}^{k+1} - (\sigma\mathbf{I} + \mathbf{Q}^{k+1})^{-1}(\nabla f(\mathbf{w}^{k+1}) + \mathbf{y}^k), \tag{4.7}$$

where $\mathbf{I}$ is an identity matrix. To ensure binary solutions eventually, we update $\mu_k$ as follows,

$$\mu_k = \mu_{k-1} + \begin{cases} \min\left\{(\eta - 1)\mu_{k-1}, \ \dfrac{\rho\sigma\|\mathbf{x}^k - \mathbf{w}^k\|^2}{\varphi(\mathbf{w}^k) + \epsilon}\right\}, & \text{if } \ \operatorname{mod}(k, k_0) = 0, \ \varphi(\mathbf{w}^k) \neq 0, \\ 0, & \text{otherwise}, \end{cases} \tag{4.8}$$

where $\eta > 1, \rho \in (0, 1/6], \ \epsilon > 0, \ k_0 > 0$ is an integer, and $\operatorname{mod}(a, b)$ returns the remainder after division of $a$ by $b$. We note that $\mathbf{w}^{k+1}$ is binary if $\varphi(\mathbf{w}^{k+1}) = 0$. In such a scenario, it is unnecessary to increase $\mu_k$ further for better solutions. The algorithm stops when $(\mathbf{w}^k, \mathbf{x}^k, \mathbf{y}^k)$ satisfies

$$\mathbf{w}^k \in \{0, 1\}^n, \quad \max\left\{\|\mathbf{x}^k - \mathbf{w}^k\|, \ \|\mathbf{y}^k + \nabla f(\mathbf{w}^k)\|\right\} < \varepsilon, \tag{4.9}$$

where $\varepsilon \in (0, 1)$ is a given tolerance. From (4.6), if $(\mathbf{w}^k, \mathbf{x}^k, \mathbf{y}^k)$ satisfies the above conditions, then $\mathbf{w}^k$ is approximately a binary P-stationary point. The proposed algorithm is presented in Algorithm 1. We term the algorithm ShaPeak, which is derived from the sharp-peak function-based ADMM.

**Algorithm 1:** (ShaPeak) Sharp-peak function-based iADMM.

**Input** $\mathbf{w}^0 = \mathbf{x}^0 \in \{0,1\}^n, \mathbf{y}^0 = -\nabla f(\mathbf{w}^0)$, and $(\mu_0, \sigma, \varepsilon) > 0$.

**for** $k = 0, 1, 2, \ldots$ **do**

  Update $(\mathbf{w}^{k+1}, \mathbf{x}^{k+1}, \mathbf{y}^{k+1})$ by (4.6), (4.7), and (4.5).

  If (4.9) holds, then stop.

  Update $\mu_{k+1}$ by (4.8).

**end**

### 4.1 Convergence analysis

Hereafter, let $\{(\mathbf{w}^k, \mathbf{x}^k, \mathbf{y}^k; \mu_k)\}$ be the sequence generated by Algorithm 1 with $\mathbf{Q}^k$ chosen as

$$\mathbf{Q}^k \succeq \mathbf{0}, \quad \|\mathbf{Q}^k\| \leqslant \lambda, \tag{4.10}$$

where $\lambda > 0$ is a predefined constant. For example, we can choose $\mathbf{Q}^k \equiv \lambda \mathbf{I}$ for problem (3.12) and $\lambda$ can be set as $\lambda = \|\mathbf{Q}\|$. Moreover, we define a useful region by

$$\Omega := \left\{ (\mathbf{w}, \mathbf{x}) \in \mathbb{B} \times \mathbb{R}^n : f(\mathbf{w}) + \frac{\sigma}{2}\|\mathbf{w} - \mathbf{x}\|^2 \leqslant f(\mathbf{w}^0) \right\}. \tag{4.11}$$

Since $f$ is continuous, it follows $f_B := \min_{\mathbf{w} \in \mathbb{B}} f(\mathbf{w}) > -\infty$, which indicates that $\Omega$ is a bounded set, thereby resulting in

$$\alpha := \frac{2f(\mathbf{w}^0) - 2f_B}{\sigma} \geqslant \|\mathbf{w} - \mathbf{x}\|^2, \quad \forall\, (\mathbf{w}, \mathbf{x}) \in \Omega. \tag{4.12}$$

To establish the convergence, we need the following assumption.

**Assumption 4.1.** *The gradient of $f$ is locally Lipschitz continuous on $\mathbb{N}$, where*

$$\mathbb{N} := \left\{ \mathbf{x} \in \mathbb{R}^n : \|\mathbf{x}\|_\infty \leqslant 1 + \frac{\sqrt{n} + \sqrt{\alpha}}{8} \right\}. \tag{4.13}$$

One can observe that $\mathbb{N}$ is a larger box than $\mathbb{B}$, namely $\mathbb{N} \supset \mathbb{B}$. According to Algorithm 1, the update of $\mathbf{x}^k$ does not involve any box constraint, making it difficult to guarantee $\mathbf{x}^k \in \mathbb{B}$. However, Lemma 4.2 1) shows that $\mathbf{x}^k$ always lies within this larger region $\mathbb{N}$. As we mentioned in Section 1.4, the local Lipschitz continuity on a compact set implies the Lipschitz continuity on this compact set. Therefore, Assumption 4.1 indicates that the gradient of $f$ is Lipschitz continuous on $\mathbb{N}$ with a constant $\beta \in (0, \infty)$, which further implies

$$f(\mathbf{w}) \leqslant f(\mathbf{x}) + \langle \nabla f(\mathbf{z}), \mathbf{w} - \mathbf{x} \rangle + \frac{\beta}{2}\|\mathbf{w} - \mathbf{x}\|^2, \quad \forall\, \mathbf{w}, \mathbf{x} \in \mathbb{N}, \ \forall\, \mathbf{z} \in \{\mathbf{w}, \mathbf{x}\}. \tag{4.14}$$

Based on two constants $\beta$ and $\lambda$, we choose $\sigma$ to satisfy

$$\sigma \geqslant 8 \max\{\lambda, \beta\}. \tag{4.15}$$

The first result shows that, under Assumption 4.1 and appropriate parameter choices, the objective function associated with $L(\mathbf{w}^k, \mathbf{x}^k, \mathbf{y}^k; \mu_k)$ is bounded below.

**Lemma 4.1.** *Suppose Assumption 4.1 holds. Let $\{(\mathbf{w}^k, \mathbf{x}^k, \mathbf{y}^k; \mu_k)\}$ be the sequence generated by Algorithm 1 with $\mathbf{Q}^k$ and $\sigma$ chosen as (4.10) and (4.15). If $\mathbf{x}^k \in \mathbb{N}$, then*

$$\begin{aligned} \widetilde{L}^k &:= L(\mathbf{w}^k, \mathbf{x}^k, \mathbf{y}^k; \mu_k) + \frac{3\sigma}{8}\|\mathbf{x}^k - \mathbf{w}^k\|^2 \\ &\geqslant f(\mathbf{w}^k) + \frac{\sigma}{2}\|\mathbf{x}^k - \mathbf{w}^k\|^2 > -\infty. \end{aligned} \tag{4.16}$$

*Proof.* For any $\mathbf{w}, \mathbf{x} \in \mathbb{R}^n$ and any $t > 0$,

$$\begin{aligned} \langle \mathbf{w}, \mathbf{x} \rangle &\leqslant (1/(2t))\|\mathbf{w}\|^2 + (t/2)\|\mathbf{x}\|^2, \\ \|\mathbf{w} + \mathbf{x}\|^2 &\leqslant (1 + 1/t)\|\mathbf{w}\|^2 + (1 + t)\|\mathbf{x}\|^2. \end{aligned} \tag{4.17}$$

Moreover, for any $k \geqslant 0$ and $\mathbf{w} \in \mathbb{R}^n$,

$$\|\mathbf{Q}^k \mathbf{w}\| \leqslant \lambda \|\mathbf{w}\| \leqslant \frac{\sigma}{8}\|\mathbf{w}\|. \tag{4.18}$$

The optimality conditions of (4.3) and (4.4) are

$$\begin{aligned} \mathbf{0} &\in \mu_k \mathbf{v}^{k+1} - \mathbf{y}^k - \sigma(\mathbf{x}^k - \mathbf{w}^{k+1}) + N_{\mathbb{B}}(\mathbf{w}^{k+1}) \\ &\in \mu_k \mathbf{v}^{k+1} - \mathbf{y}^{k+1} + \sigma(\mathbf{x}^{k+1} - \mathbf{x}^k) + N_{\mathbb{B}}(\mathbf{w}^{k+1}), && (4.19) \\ \mathbf{0} &= \nabla f(\mathbf{w}^{k+1}) + \mathbf{y}^k + (\sigma \mathbf{I} + \mathbf{Q}^{k+1})(\mathbf{x}^{k+1} - \mathbf{w}^{k+1}) && (4.20) \\ &= \nabla f(\mathbf{w}^{k+1}) + \mathbf{y}^{k+1} + \mathbf{Q}^{k+1}(\mathbf{x}^{k+1} - \mathbf{w}^{k+1}), && (4.21) \end{aligned}$$

where $\mathbf{v}^{k+1} \in \varphi(\mathbf{w}^{k+1})$ and (4.19) and (4.21) result from (4.5). By Algorithm 1, $\mathbf{w}^k \in \mathbb{B}$ and thus $\varphi(\mathbf{w}^k) \geqslant 0$, thereby deriving that

$$\begin{aligned} \widetilde{L}^k &= f(\mathbf{x}^k) + \mu_k \varphi(\mathbf{w}^k) + \langle \mathbf{y}^k, \mathbf{x}^k - \mathbf{w}^k \rangle + \frac{7\sigma}{8}\|\mathbf{x}^k - \mathbf{w}^k\|^2 \\ &\geqslant f(\mathbf{w}^k) + \langle \nabla f(\mathbf{w}^k) + \mathbf{y}^k, \mathbf{x}^k - \mathbf{w}^k \rangle + \frac{7\sigma - 4\beta}{8}\|\mathbf{x}^k - \mathbf{w}^k\|^2 \\ &\geqslant f(\mathbf{w}^k) - \langle \mathbf{Q}^k(\mathbf{x}^k - \mathbf{w}^k), \mathbf{x}^k - \mathbf{w}^k \rangle + \frac{13\sigma}{16}\|\mathbf{x}^k - \mathbf{w}^k\|^2 \\ &\geqslant f(\mathbf{w}^k) - \frac{1}{\sigma}\|\mathbf{Q}^k(\mathbf{x}^k - \mathbf{w}^k)\|^2 + \frac{9\sigma}{16}\|\mathbf{x}^k - \mathbf{w}^k\|^2 \\ &\geqslant f(\mathbf{w}^k) + \frac{\sigma}{2}\|\mathbf{x}^k - \mathbf{w}^k\|^2 \\ &\geqslant f_B > -\infty, \end{aligned}$$

where the first inequality is from $\mathbf{x}^k \in \mathbb{N}$ and (4.14) by Assumption 4.1, the second inequality is due to (4.21) and (4.15), the third and fourth inequalities hold by (4.17) and (4.18), and the fifth inequality is because of $\mathbf{w}^k \in \mathbb{B}$ and $f_B = \min_{\mathbf{w} \in \mathbb{B}} f(\mathbf{w})$. □

Based on the above lemma, we next prove that sequence $\{(\mathbf{w}^k, \mathbf{x}^k)\}$ is bounded in $\Omega \cap (\mathbb{B} \times \mathbb{N})$ and sequence $\{\widetilde{L}^k\}$ is strictly increasing under the same conditions.

**Lemma 4.2.** *Suppose Assumption 4.1 holds. Let $\{(\mathbf{w}^k, \mathbf{x}^k, \mathbf{y}^k; \mu_k)\}$ be the sequence generated by Algorithm 1 with $\mathbf{Q}^k$ and $\sigma$ chosen as (4.10) and (4.15). The following results hold.*

*1) For any $k \geqslant 0$, $(\mathbf{w}^k, \mathbf{x}^k) \in \Omega \cap (\mathbb{B} \times \mathbb{N})$;*

*2) For any $k \geqslant 0$,*

$$\widetilde{L}^{k+1} - \widetilde{L}^k \leqslant -\frac{\sigma}{8}\|\mathbf{x}^{k+1} - \mathbf{x}^k\|^2. \tag{4.22}$$

*Proof.* We prove 1) and 2) together. By (4.8), if $\mathrm{mod}(k+1, k_0) = 0$ and $\varphi(\mathbf{w}^{k+1}) \neq 0$, then

$$(\mu_{k+1} - \mu_k)\varphi(\mathbf{w}^{k+1}) \leqslant \rho\sigma\|\mathbf{x}^{k+1} - \mathbf{w}^{k+1}\|^2 \leqslant \frac{1}{6\sigma}\|\mathbf{y}^{k+1} - \mathbf{y}^k\|^2. \tag{4.23}$$

where the last inequality is due to $\rho \in (0, 1/6]$ and (4.5). Otherwise $\mu_{k+1} = \mu_k$. Therefore, both cases yield the above fact. Moreover, as $\mathbf{w}^k \in \mathbb{B} \subset \mathbb{N}$ for any $k \geqslant 0$, Assumption 4.1 indicates

$$\|\nabla f(\mathbf{w}^{k+1}) - \nabla f(\mathbf{w}^k)\| \leqslant \beta\|\mathbf{w}^{k+1} - \mathbf{w}^k\| \leqslant \frac{\sigma}{8}\|\mathbf{w}^{k+1} - \mathbf{w}^k\|, \tag{4.24}$$

where the last inequality is by (4.15). By denoting

$$\phi^{k+1} := \|\mathbf{x}^k - \mathbf{w}^k\|^2 - \|\mathbf{x}^{k+1} - \mathbf{w}^{k+1}\|^2, \tag{4.25}$$

it follows from (4.21) that

$$\begin{aligned}
\|\mathbf{y}^{k+1} - \mathbf{y}^k\|^2 &= \|\nabla f(\mathbf{w}^{k+1}) - \nabla f(\mathbf{w}^k) + \mathbf{Q}^{k+1}(\mathbf{x}^{k+1} - \mathbf{w}^{k+1}) - \mathbf{Q}^k(\mathbf{x}^k - \mathbf{w}^k)\|^2 \\
&\leqslant \frac{4}{3}\|\nabla f(\mathbf{w}^{k+1}) - \nabla f(\mathbf{w}^k)\|^2 + 8\|\mathbf{Q}^{k+1}(\mathbf{x}^{k+1} - \mathbf{w}^{k+1})\|^2 + 8\|\mathbf{Q}^k(\mathbf{x}^k - \mathbf{w}^k)\|^2 \\
&\leqslant \frac{\sigma^2}{48}\|\mathbf{w}^{k+1} - \mathbf{w}^k\|^2 + \frac{\sigma^2}{8}\|\mathbf{x}^{k+1} - \mathbf{w}^{k+1}\|^2 + \frac{\sigma^2}{8}\|\mathbf{x}^k - \mathbf{w}^k\|^2 \\
&\leqslant \frac{\sigma^2}{16}\|\mathbf{x}^{k+1} - \mathbf{x}^k\|^2 + \frac{3\sigma^2}{16}\|\mathbf{x}^{k+1} - \mathbf{w}^{k+1}\|^2 + \frac{3\sigma^2}{16}\|\mathbf{x}^k - \mathbf{w}^k\|^2 \\
&= \frac{\sigma^2}{16}\|\mathbf{x}^{k+1} - \mathbf{x}^k\|^2 + \frac{3\sigma^2}{16}\phi^{k+1} + \frac{3\sigma^2}{8}\|\mathbf{x}^{k+1} - \mathbf{w}^{k+1}\|^2 \\
&= \frac{\sigma^2}{16}\|\mathbf{x}^{k+1} - \mathbf{x}^k\|^2 + \frac{3\sigma^2}{16}\phi^{k+1} + \frac{3}{8}\|\mathbf{y}^{k+1} - \mathbf{y}^k\|^2,
\end{aligned} \tag{4.26}$$

where the first inequality is from (4.17), the second inequality is from (4.24) and (4.18), the third inequality is from (4.15), and the last inequality is from $\|\mathbf{w}^{k+1} - \mathbf{w}^k\|^2 \leqslant 3\|\mathbf{w}^{k+1} - \mathbf{x}^{k+1}\|^2 + 3\|\mathbf{x}^{k+1} - \mathbf{x}^k\|^2 + 3\|\mathbf{x}^k - \mathbf{w}^k\|^2$. The above condition results in

$$\|\mathbf{y}^{k+1} - \mathbf{y}^k\|^2 \leqslant \frac{\sigma^2}{10}\|\mathbf{x}^{k+1} - \mathbf{x}^k\|^2 + \frac{3\sigma^2}{10}\phi^{k+1}. \tag{4.27}$$

We now decompose a gap $G^{k+1}$ by

$$G^{k+1} := L(\mathbf{w}^{k+1}, \mathbf{x}^{k+1}, \mathbf{y}^{k+1}; \mu_{k+1}) - L(\mathbf{w}^k, \mathbf{x}^k, \mathbf{y}^k; \mu_k) = G_\mu^{k+1} + G_\mathbf{y}^{k+1} + G_\mathbf{x}^{k+1} + G_\mathbf{w}^{k+1},$$

where $G_\mu^{k+1}, G_\mathbf{y}^{k+1}, G_\mathbf{x}^{k+1}$, and $G_\mathbf{w}^{k+1}$ are defined by

$$\begin{aligned}
G_\mu^{k+1} &:= L(\mathbf{w}^{k+1}, \mathbf{x}^{k+1}, \mathbf{y}^{k+1}; \mu_{k+1}) - L(\mathbf{w}^{k+1}, \mathbf{x}^{k+1}, \mathbf{y}^{k+1}; \mu_k), \\
G_\mathbf{y}^{k+1} &:= L(\mathbf{w}^{k+1}, \mathbf{x}^{k+1}, \mathbf{y}^{k+1}; \mu_k) - L(\mathbf{w}^{k+1}, \mathbf{x}^{k+1}, \mathbf{y}^k; \mu_k), \\
G_\mathbf{x}^{k+1} &:= L(\mathbf{w}^{k+1}, \mathbf{x}^{k+1}, \mathbf{y}^k; \mu_k) - L(\mathbf{w}^{k+1}, \mathbf{x}^k, \mathbf{y}^k; \mu_k), \\
G_\mathbf{w}^{k+1} &:= L(\mathbf{w}^{k+1}, \mathbf{x}^k, \mathbf{y}^k; \mu_k) - L(\mathbf{w}^k, \mathbf{x}^k, \mathbf{y}^k; \mu_k).
\end{aligned}$$

Using (4.23) and (4.5), one can check that

$$G_\mu^{k+1} = (\mu_{k+1} - \mu_k)\varphi(\mathbf{w}^{k+1}) \leqslant \frac{1}{6\sigma}\|\mathbf{y}^{k+1} - \mathbf{y}^k\|^2 \tag{4.28}$$

$$G_\mathbf{y}^{k+1} = \langle \mathbf{y}^{k+1} - \mathbf{y}^k, \mathbf{x}^{k+1} - \mathbf{w}^{k+1}\rangle = \frac{1}{\sigma}\|\mathbf{y}^{k+1} - \mathbf{y}^k\|^2. \tag{4.29}$$

In the sequel, we aim to estimate $G_\mathbf{x}^{k+1}$ and $G_\mathbf{w}^{k+1}$ so as to estimate gap $G^{k+1}$ by induction.

For $k=0$, $(\mathbf{w}^0,\mathbf{x}^0)\in\Omega$ because $\mathbf{w}^0=\mathbf{x}^0\in\{0,1\}^n\subseteq\mathbb{B}$ in Algorithm 1. Note that $\mathbf{y}^0=-\nabla f(\mathbf{w}^0)$ and $\mathbf{w}^0=\mathbf{x}^0$, which means that (4.21) holds for $k=0$. This together with (4.7) leads to

$$\begin{aligned}
\|\mathbf{x}^1\|_\infty &= \|\mathbf{w}^1-(\sigma\mathbf{I}+\mathbf{Q}^1)^{-1}(\nabla f(\mathbf{w}^1)+\mathbf{y}^0)\|_\infty\\
&= \|\mathbf{w}^1-(\sigma\mathbf{I}+\mathbf{Q}^1)^{-1}(\nabla f(\mathbf{w}^1)-\nabla f(\mathbf{w}^0)+\mathbf{Q}^0(\mathbf{x}^0-\mathbf{w}^0))\|_\infty\\
&\leqslant \|\mathbf{w}^1\|_\infty+\|(\sigma\mathbf{I}+\mathbf{Q}^1)^{-1}(\nabla f(\mathbf{w}^1)-\nabla f(\mathbf{w}^0)+\mathbf{Q}^0(\mathbf{x}^0-\mathbf{w}^0))\|\\
&\leqslant 1+\|(\sigma\mathbf{I}+\mathbf{Q}^1)^{-1}\|(\|\nabla f(\mathbf{w}^1)-\nabla f(\mathbf{w}^0)\|+\|\mathbf{Q}^0(\mathbf{x}^0-\mathbf{w}^0)\|)\\
&\leqslant 1+(\beta/\sigma)\|\mathbf{w}^1-\mathbf{w}^0\|+(\lambda/\sigma)\|\mathbf{x}^0-\mathbf{w}^0\|\\
&\leqslant 1+(1/8)\|\mathbf{w}^1-\mathbf{w}^0\|+(1/8)\|\mathbf{x}^0-\mathbf{w}^0\|\\
&\leqslant 1+(\sqrt{n}+\sqrt{\alpha})/8,
\end{aligned}\tag{4.30}$$

where the second equality is from (4.21) with $k=0$, the first inequality is because of $\|\mathbf{w}\|_\infty\leqslant\|\mathbf{w}\|$, the third inequality is from (4.24) and (4.18), the fourth inequality is from (4.15), and the last inequality is due to $\mathbf{w}^0,\mathbf{w}^1\in\mathbb{B}$ and (4.12) (because of $(\mathbf{w}^0,\mathbf{x}^0)\in\Omega$). Therefore, $(\mathbf{w}^1,\mathbf{x}^1)\in\mathbb{B}\times\mathbb{N}$, which by $\mathbf{x}^0\in\mathbb{N}$, Assumption 4.1, and (4.14) derives that

$$f(\mathbf{x}^1)\leqslant f(\mathbf{x}^0)+\langle\nabla f(\mathbf{x}^1),\mathbf{x}^1-\mathbf{x}^0\rangle+\frac{\beta}{2}\|\mathbf{x}^1-\mathbf{x}^0\|^2.$$

This allows us to obtain the following chain of inequalities,

$$\begin{aligned}
G^1_{\mathbf{x}} &= f(\mathbf{x}^1)-f(\mathbf{x}^0)+\langle\mathbf{y}^0,\mathbf{x}^1-\mathbf{x}^0\rangle+\frac{\sigma}{2}\left(\|\mathbf{x}^1-\mathbf{w}^1\|^2-\|\mathbf{x}^0-\mathbf{w}^1\|^2\right)\\
&\leqslant -\frac{\sigma-\beta}{2}\|\mathbf{x}^1-\mathbf{x}^0\|^2+\langle\nabla f(\mathbf{x}^1)+\mathbf{y}^0+\sigma(\mathbf{x}^1-\mathbf{w}^1),\mathbf{x}^1-\mathbf{x}^0\rangle\\
&\leqslant -\frac{7\sigma}{16}\|\mathbf{x}^1-\mathbf{x}^0\|^2+\langle\nabla f(\mathbf{x}^1)-\nabla f(\mathbf{w}^1)-\mathbf{Q}^1(\mathbf{x}^1-\mathbf{w}^1),\mathbf{x}^1-\mathbf{x}^0\rangle\\
&\leqslant -\frac{\sigma}{4}\|\mathbf{x}^1-\mathbf{x}^0\|^2+\frac{4}{3\sigma}\|\nabla f(\mathbf{x}^1)-\nabla f(\mathbf{w}^1)-\mathbf{Q}^1(\mathbf{x}^1-\mathbf{w}^1)\|^2\\
&\leqslant -\frac{\sigma}{4}\|\mathbf{x}^1-\mathbf{x}^0\|^2+\frac{8\beta^2}{3\sigma}\|\mathbf{x}^1-\mathbf{w}^1\|^2+\frac{8\lambda^2}{3\sigma}\|\mathbf{x}^1-\mathbf{w}^1\|^2\\
&\leqslant -\frac{\sigma}{4}\|\mathbf{x}^1-\mathbf{x}^0\|^2+\frac{\sigma}{12}\|\mathbf{x}^1-\mathbf{w}^1\|^2\\
&\leqslant -\frac{\sigma}{4}\|\mathbf{x}^1-\mathbf{x}^0\|^2+\frac{1}{12\sigma}\|\mathbf{y}^1-\mathbf{y}^0\|^2,
\end{aligned}\tag{4.31}$$

where the second inequality is from (4.15) and (4.20), the third inequality is from (4.17), the fourth inequality is due to $\mathbf{w}^1,\mathbf{x}^1\in\mathbb{N}$ and Assumption 4.1 and (4.18), the fifth inequality is by (4.15), and the last inequality is from (4.5). Finally, the optimality of $\mathbf{w}^1$ to problem (4.6) suffices to

$$G^1_{\mathbf{w}}=\mu_0\varphi(\mathbf{w}^1)-\langle\mathbf{y}^0,\mathbf{w}^1\rangle+\frac{\sigma}{2}\|\mathbf{x}^0-\mathbf{w}^1\|^2-\left(\mu_0\varphi(\mathbf{w}^0)-\langle\mathbf{y}^0,\mathbf{w}^0\rangle+\frac{\sigma}{2}\|\mathbf{x}^0-\mathbf{w}^0\|^2\right)\leqslant 0.\tag{4.32}$$

Combining (4.28), (4.29), (4.31), and (4.32) derives that

$$\begin{aligned}
G^1 &\leqslant -\frac{\sigma}{4}\|\mathbf{x}^1-\mathbf{x}^0\|^2+\frac{5}{4\sigma}\|\mathbf{y}^1-\mathbf{y}^0\|^2\\
&\leqslant -\frac{\sigma}{8}\|\mathbf{x}^1-\mathbf{x}^0\|^2+\frac{3\sigma}{8}\phi^1,
\end{aligned}$$

where the last inequality is from (4.27). The above condition can show (4.22) with $k=0$, namely,

$$\widetilde{L}^1-\widetilde{L}^0\leqslant -\frac{\sigma}{8}\|\mathbf{x}^1-\mathbf{x}^0\|^2,\tag{4.33}$$

For $k=1$, we first prove $(\mathbf{w}^1,\mathbf{x}^1)\in\Omega$. Based on the initialization of Algorithm 1, there is

$$\widetilde{L}^0 = f(\mathbf{w}^0).$$

In addition, we have shown $\mathbf{x}^1\in\mathbb{N}$, which recalls (4.16) and (4.33) derives

$$f(\mathbf{w}^1)+\frac{\sigma}{2}\|\mathbf{x}^1-\mathbf{w}^1\|^2 \leqslant \widetilde{L}^1 \leqslant \widetilde{L}^0 = f(\mathbf{w}^0).$$

As a result of the above condition and (4.11), we obtain $(\mathbf{w}^1,\mathbf{x}^1)\in\Omega$, thereby resulting in

$$(\mathbf{w}^1,\mathbf{x}^1)\in\Omega\cap(\mathbb{B}\times\mathbb{N}).$$

Then the similar reasoning to prove $\mathbf{x}^1\in\mathbb{N}$ (see (4.30)) and (4.33) enables showing $\mathbf{x}^2\in\mathbb{N}$ and

$$\widetilde{L}^2-\widetilde{L}^1 \leqslant -\frac{\sigma}{8}\|\mathbf{x}^1-\mathbf{x}^2\|^2.$$

For $k\geqslant 2$, repeating the above proof enables the establishment of the results. □

Using the above lemma, the following theorem establishes the global convergence of Algorithm 1, showing that any accumulation point of $\{\mathbf{x}^k\}$ is a P-stationary point of a new penalty model $\min_{\mathbf{x}\in\mathbb{B}} F(\mathbf{x};\mu_\infty)$, where $\mu_\infty$ is the limit of $\{\mu_k\}$. As stated in Theorem 3.3, P-stationary points are closely related to local/global minimizers. To obtain a stronger convergence property (i.e., the whole sequence converges to a P-stationary point), an additional condition on final penalty parameter $\mu_\infty$ is imposed, that is, $\mu_\infty>\overline{\mu}$. This condition can be ensured if initializing $\mu_0$ as $\mu_0>\overline{\mu}$ due to $\mu_\infty\geqslant\mu_0$ from (4.8).

**Theorem 4.1.** *Suppose Assumption 4.1 holds. Let $\{(\mathbf{w}^k,\mathbf{x}^k,\mathbf{y}^k;\mu_k)\}$ be the sequence generated by Algorithm 1 with $\mathbf{Q}^k$ and $\sigma$ chosen as (4.10) and (4.15). The following results hold.*

*1) $\{L(\mathbf{w}^k,\mathbf{x}^k,\mathbf{y}^k;\mu_k)\}$ and $\{\widetilde{L}^k\}$ converge to the same value, $\{\mu_k\}$ converges (to $\mu_\infty$), and*

$$\lim_{k\to\infty}\|\mathbf{w}^{k+1}-\mathbf{w}^k\| = \lim_{k\to\infty}\|\mathbf{x}^{k+1}-\mathbf{x}^k\| = \lim_{k\to\infty}\|\mathbf{y}^{k+1}-\mathbf{y}^k\| = \lim_{k\to\infty}\|\mathbf{w}^k-\mathbf{x}^k\| = 0.$$

*2) Any accumulation point of $\{\mathbf{x}^k\}$ is a P-stationary point $\mathbf{x}^\infty$ with $1/\sigma$ of problem $\min_{\mathbf{x}\in\mathbb{B}} F(\mathbf{x};\mu_\infty)$.*

*3) Sequence $\{\mathbf{x}^k\}$ converges to a binary P-stationary point $\mathbf{x}^\infty$ if $\mu_\infty>\overline{\mu}$.*

*Proof.* 1) From (4.22), sequence $\{\widetilde{L}^k\}$ is non-increasing. Moreover, from (4.16), for any $k\geqslant 0$,

$$\widetilde{L}^k \geqslant f(\mathbf{w}^k)+\frac{\sigma}{2}\|\mathbf{x}^k-\mathbf{w}^k\|^2 \geqslant f_B.$$

Therefore, sequence $\{\widetilde{L}^k\}$ converges. Again by (4.22) and $\widetilde{L}^0=f(\mathbf{w}^0)$, for any $\ell\geqslant k\geqslant 0$,

$$\sum_{k=0}^{\ell-1}\frac{\sigma}{8}\|\mathbf{x}^{k+1}-\mathbf{x}^k\|^2 \leqslant \sum_{k=0}^{\ell-1}(\widetilde{L}^k-\widetilde{L}^{k+1}) = \widetilde{L}^0-\widetilde{L}^\ell \leqslant f(\mathbf{w}^0)-f_B. \tag{4.34}$$

The above condition implies $\lim_{k\to\infty}\|\mathbf{x}^{k+1}-\mathbf{x}^k\|=0$. It follows from (4.26) that

$$\begin{aligned}\|\mathbf{y}^{k+1}-\mathbf{y}^k\|^2 &\leqslant \frac{\sigma^2}{16}\|\mathbf{x}^{k+1}-\mathbf{x}^k\|^2+\frac{3\sigma^2}{16}\|\mathbf{x}^{k+1}-\mathbf{w}^{k+1}\|^2+\frac{3\sigma^2}{16}\|\mathbf{x}^k-\mathbf{w}^k\|^2\\ &= \frac{\sigma^2}{16}\|\mathbf{x}^{k+1}-\mathbf{x}^k\|^2+\frac{3}{16}\|\mathbf{y}^{k+1}-\mathbf{y}^k\|^2+\frac{3}{16}\|\mathbf{y}^k-\mathbf{y}^{k-1}\|^2,\end{aligned}$$

where the equality is from (4.5), which results in

$$\sum_{k=0}^{\ell-1} 13\|\mathbf{y}^{k+1}-\mathbf{y}^k\|^2 \leqslant \sum_{k=0}^{\ell-1} \sigma^2\|\mathbf{x}^{k+1}-\mathbf{x}^k\|^2 + \sum_{k=0}^{\ell-1} 3\|\mathbf{y}^k-\mathbf{y}^{k-1}\|^2.$$

This further gives rise to

$$\begin{aligned}\sum_{k=0}^{\ell-1} 10\|\mathbf{y}^{k+1}-\mathbf{y}^k\|^2 &\leqslant 13\|\mathbf{y}^{\ell}-\mathbf{y}^{\ell-1}\|^2 + \sum_{k=0}^{\ell-1} 10\|\mathbf{y}^k-\mathbf{y}^{k-1}\|^2 \\ &= \sum_{k=0}^{\ell-1} 13\|\mathbf{y}^{k+1}-\mathbf{y}^k\|^2 - \sum_{k=0}^{\ell-1} 3\|\mathbf{y}^k-\mathbf{y}^{k-1}\|^2 \\ &\leqslant \sum_{k=0}^{\ell-1} \sigma^2\|\mathbf{x}^{k+1}-\mathbf{x}^k\|^2 \\ &\leqslant 8\sigma(f(\mathbf{w}^0)-f_B), \end{aligned} \tag{4.35}$$

where the last inequality is due to (4.34). In the above inequalities, we let $\mathbf{y}^{-1}=\mathbf{y}^0$. The above condition implies $\|\mathbf{y}^{k+1}-\mathbf{y}^k\| \to 0$ as $k\to\infty$, which by (4.5) derives $\|\mathbf{x}^{k+1}-\mathbf{w}^{k+1}\| \to 0$. This and (4.16) yield $\widetilde{L}^k - L(\mathbf{w}^k,\mathbf{x}^k,\mathbf{y}^k;\mu_k) \to 0$. Finally,

$$\|\mathbf{w}^{k+1}-\mathbf{w}^k\| = \|\mathbf{w}^{k+1}-\mathbf{x}^{k+1}+\mathbf{x}^{k+1}-\mathbf{x}^k+\mathbf{x}^k-\mathbf{w}^k\| \to 0.$$

It is follows from (4.8) that if $\mathrm{mod}(k+1,k_0)=0$ and $\varphi(\mathbf{w}^{k+1})\neq 0$, then

$$\mu_{k+1}-\mu_k \leqslant \frac{\rho\sigma}{\epsilon}\|\mathbf{x}^{k+1}-\mathbf{w}^{k+1}\|^2 \leqslant \frac{1}{6\epsilon\sigma}\|\mathbf{y}^{k+1}-\mathbf{y}^k\|^2.$$

Otherwise $\mu_{k+1}=\mu_k$. Therefore, both cases result in the above condition. Then

$$\mu_\ell-\mu_0 = \sum_{k=0}^{\ell-1}(\mu_{k+1}-\mu_k) \leqslant \sum_{k=0}^{\ell-1}\frac{1}{6\epsilon\sigma}\|\mathbf{y}^{k+1}-\mathbf{y}^k\|^2 \leqslant \frac{2(f(\mathbf{w}^0)-f_B)}{15\epsilon},$$

where the last inequality is from (4.35). The above condition means that sequence $\{\mu_k\}$ is bounded from above, which by (4.8) that it is non-decreasing shows its convergence.

2) Let $(\mathbf{w}^\infty,\mathbf{x}^\infty,\mathbf{y}^\infty;\mu_\infty)$ be an accumulation point of sequence $\{(\mathbf{w}^k,\mathbf{x}^k,\mathbf{y}^k;\mu_k)\}$, namely, there is a subset $\mathcal{K}\subseteq\{1,2,3,\ldots\}$ such that $\lim_{k\in\mathcal{K},k\to\infty}(\mathbf{w}^k,\mathbf{x}^k,\mathbf{y}^k;\mu_k)=(\mathbf{w}^\infty,\mathbf{x}^\infty,\mathbf{y}^\infty;\mu_\infty)$. Clearly, $\mathbf{w}^\infty=\mathbf{x}^\infty$ due to claim 1). Then taking the limit of the right-hand side of (4.21) along with $k\in\mathcal{K}$ results in $\mathbf{y}^\infty=-\nabla f(\mathbf{w}^\infty)=-\nabla f(\mathbf{x}^\infty)$. It is observed from (4.6) that

$$\mathbf{w}^{k+1}\in \mathrm{Prox}^{\mathbb{B}}_{(\mu_k/\sigma)\varphi}(\mathbf{x}^k+\mathbf{y}^k/\sigma) = \mathrm{Prox}_{(\mu_k/\sigma)(\varphi+\delta_{\mathbb{B}})}(\mathbf{x}^k+\mathbf{y}^k/\sigma).$$

Using [27, Theorem 1.25], taking the limit of both sides of the above inclusion along with $k\in\mathcal{K}$ yields the following inclusion,

$$\begin{aligned}\mathbf{x}^\infty=\mathbf{w}^\infty &\in \mathrm{Prox}_{(\mu_\infty/\sigma)(\varphi+\delta_{\mathbb{B}})}\left(\mathbf{x}^\infty+\mathbf{y}^\infty/\sigma\right) \\ &= \mathrm{Prox}_{(\mu_\infty/\sigma)(\varphi+\delta_{\mathbb{B}})}\left(\mathbf{x}^\infty-\nabla f(\mathbf{x}^\infty)/\sigma\right) \\ &= \mathrm{Prox}^{\mathbb{B}}_{(\mu_\infty/\sigma)\varphi}\left(\mathbf{x}^\infty-\nabla f(\mathbf{x}^\infty)/\sigma\right).\end{aligned}$$

Therefore, $\mathbf{x}^\infty$ is a P-stationary point with $1/\sigma$ of problem $\min_{\mathbf{x}\in\mathbb{B}} F(\mathbf{x};\mu_\infty)$.

3) Based on Theorems 3.3 and 3.1, a P-stationary point is a KKT point that is binary. Hence, $\mathbf{x}^\infty\in\{0,1\}^n$. This means that $\mathbf{x}^\infty$ is isolated, which together with $\lim_{k\to\infty}\|\mathbf{x}^{k+1}-\mathbf{x}^k\|=0$ and [21, Lemma 4.10] delivers the whole sequence convergence. □

Finally, under an additional condition on the initialization of $\mu_0$, we establish the local convergence rate. As outlined below, sequence $\mathbf{x}^k$ converges to its binary limit point $\mathbf{x}^\infty$, which is also a P-stationary point of problem $\min_{\mathbf{x}\in\mathbb{B}} F(\mathbf{x};\mu_\infty)$, in a linear rate, and sequence $\{\mathbf{w}^k\}$ eventually coincides with this limit, namely, $\mathbf{w}^k \equiv \mathbf{x}^\infty$.

**Theorem 4.2.** *Suppose Assumption 4.1 holds. Let $\{(\mathbf{w}^k, \mathbf{x}^k, \mathbf{y}^k; \mu_k)\}$ be the sequence generated by Algorithm 1 with $\mathbf{Q}^k$ and $\sigma$ chosen as (4.10) and (4.15), and $\mu_0$ chosen as*

$$\mu_0 > \overline{\mu} + \frac{\sigma(\sqrt{\alpha}+1)}{c}. \tag{4.36}$$

*Then there is an integer $\kappa > 0$ such that for any $k \geqslant \kappa$,*

$$\begin{aligned} \mathbf{w}^{k+1} \equiv \mathbf{w}^k \equiv \mathbf{x}^\infty &\in \{0,1\}^n, \\ \|\mathbf{x}^k - \mathbf{x}^\infty\| &\leqslant \sqrt{\alpha}\gamma^{k-\kappa}, \\ \|\mathbf{y}^k + \nabla f(\mathbf{x}^\infty)\| &\leqslant \sqrt{\alpha}\lambda\gamma^{k-\kappa}, \end{aligned} \tag{4.37}$$

*where $\gamma := \lambda/(\sigma-\lambda) \in (0, 1/7]$. Consequently, after the following number of iterations,*

$$\kappa + \left\lceil \log_\gamma \left( \frac{\varepsilon}{\max\{1,\lambda\}\sqrt{\alpha}} \right) \right\rceil, \tag{4.38}$$

*stopping conditions in (4.9) can be satisfied, where $\lceil a \rceil$ is the ceiling of $a$.*

*Proof.* Direct verification leads to

$$\begin{aligned} \|\mathbf{y}^k + \sigma(\mathbf{x}^k - \mathbf{w}^{k+1})\|_\infty &= \| -\nabla f(\mathbf{w}^k) - \mathbf{Q}^k(\mathbf{x}^k - \mathbf{w}^k) + \sigma(\mathbf{x}^k - \mathbf{w}^{k+1})\|_\infty \\ &= \| -\nabla f(\mathbf{w}^k) + (\sigma\mathbf{I} - \mathbf{Q}^k)(\mathbf{x}^k - \mathbf{w}^k) + \sigma(\mathbf{w}^k - \mathbf{w}^{k+1})\|_\infty \\ &\leqslant \|\nabla f(\mathbf{w}^k)\|_\infty + \|(\sigma\mathbf{I} - \mathbf{Q}^k)(\mathbf{x}^k - \mathbf{w}^k)\|_\infty + \|\sigma(\mathbf{w}^k - \mathbf{w}^{k+1})\|_\infty \\ &\leqslant c\overline{\mu} + \|(\sigma\mathbf{I} - \mathbf{Q}^k)(\mathbf{x}^k - \mathbf{w}^k)\| + \sigma \\ &\leqslant c\overline{\mu} + \sigma\|\mathbf{x}^k - \mathbf{w}^k\| + \sigma \\ &\leqslant c\overline{\mu} + \sigma(\sqrt{\alpha}+1), \end{aligned} \tag{4.39}$$

where the first equality is from (4.21), the second inequality is because of $\mathbf{w}^k, \mathbf{w}^{k+1} \in \mathbb{B}$, (3.1), and $\|\mathbf{w}\|_\infty \leqslant \|\mathbf{w}\|$, and the last inequality holds due to $(\mathbf{w}^k, \mathbf{x}^k) \in \Omega$ and (4.12). Suppose that there is $i$ such that $w_i^{k+1} \in (0,1)$. Then condition (4.19) indicates that

$$\mu_k v_i^{k+1} - y_i^k - \sigma(x_i^k - w_i^{k+1}) = 0,$$

which leads to

$$\begin{aligned} \mu_k \leqslant \frac{|\mu_k v_i^{k+1}|}{c} &= \frac{|y_i^k + \sigma(x_i^k - w_i^{k+1})|}{c} \\ &\leqslant \frac{\|\mathbf{y}^k + \sigma(\mathbf{x}^k - \mathbf{w}^{k+1})\|_\infty}{c} \\ &\leqslant \overline{\mu} + \frac{\sigma(\sqrt{\alpha}+1)}{c}. \end{aligned}$$

where the first inequality is due to $\mathbf{v}^{k+1} \in \varphi(\mathbf{w}^{k+1})$ and (2.1). This contradicts (4.36). Therefore, we must have $\mathbf{w}^k \in \{0,1\}^n$ for any $k \geqslant 1$. As $\lim_{k\to\infty} \|\mathbf{w}^{k+1} - \mathbf{w}^k\| = 0$, there is an integer $\kappa > 0$ such that for any $k \geqslant \kappa$,

$$\mathbf{w}^{k+1} \equiv \mathbf{w}^k \in \{0,1\}^n.$$

Since $\mu_\infty \geqslant \mu_0 > \overline{\mu}$ from (4.8), and (4.36), sequence $\{\mathbf{x}^k\}$ converges to a P-stationary point denoted by $\mathbf{x}^\infty$ by Theorem 4.1 3). This indicates that $\mathbf{w}^k \to \mathbf{x}^\infty$ due to $\|\mathbf{x}^k - \mathbf{w}^k\| \to 0$ and $\mathbf{y}^k \to -\nabla f(\mathbf{x}^\infty)$ due to (4.21). Therefore, we have

$$\mathbf{w}^{k+1} \equiv \mathbf{w}^k \equiv \mathbf{x}^\infty \in \{0,1\}^n, \quad \forall\, k \geqslant \kappa. \tag{4.40}$$

This condition and (4.21) enable us to obtain that for any $k \geqslant \kappa$,

$$\begin{aligned}\sigma\|\mathbf{x}^{k+1} - \mathbf{w}^{k+1}\| = \|\mathbf{y}^{k+1} - \mathbf{y}^k\| &= \|\mathbf{Q}^{k+1}(\mathbf{x}^{k+1} - \mathbf{w}^{k+1}) - \mathbf{Q}^k(\mathbf{x}^k - \mathbf{w}^k)\| \\ &\leqslant \lambda\|\mathbf{x}^{k+1} - \mathbf{w}^{k+1}\| + \lambda\|\mathbf{x}^k - \mathbf{w}^k\|,\end{aligned}$$

which immediately results in

$$\|\mathbf{x}^{k+1} - \mathbf{w}^{k+1}\| \leqslant \gamma\|\mathbf{x}^k - \mathbf{w}^k\|.$$

where $\gamma = \lambda/(\sigma - \lambda) \in (0, 1/7]$ due to (4.15). This further yields that

$$\|\mathbf{x}^k - \mathbf{w}^k\| \leqslant \gamma\|\mathbf{x}^{k-1} - \mathbf{w}^{k-1}\| \leqslant \cdots \leqslant \gamma^{k-\kappa}\|\mathbf{x}^\kappa - \mathbf{w}^\kappa\| \leqslant \sqrt{\alpha}\gamma^{k-\kappa},$$

where the last inequality is from $(\mathbf{w}^k, \mathbf{x}^k) \in \Omega$ for any $k \geqslant 0$ and (4.12). The above condition and (4.21) allow us to derive that

$$\|\nabla f(\mathbf{w}^k) + \mathbf{y}^k\| \leqslant \|\mathbf{Q}^k(\mathbf{x}^k - \mathbf{w}^k)\| \leqslant \sqrt{\alpha}\lambda\gamma^{k-\kappa}.$$

Using (4.40) and replacing $\mathbf{w}^k$ by $\mathbf{x}^\infty$ in the above two conditions show (4.37). Finally, based on (4.37), it is easy to verify that conditions in (4.9) can be satisfied after the $t$th iteration, where $t$ is the number defined in (4.38). □

# 5 Numerical experiment

In this section, we test ShaPeak on solving three problems: the recovery problems, the Multiple-Input-Multiple-Output (MIMO) detection, and the quadratic unconstrained binary optimization (QUBO). All codes are implemented in MATLAB (R2021a) on a desktop computer equipped with an Intel(R) Xeon W-3465X CPU (2.50 GHz) and 128 GB of RAM.

## 5.1 Recovery problem

The problem is to recover a signal $\mathbf{x}^*$ from a linear model $\mathbf{b} = \mathbf{A}\mathbf{x}^* + \boldsymbol{\varepsilon}$, where $\mathbf{A} \in \mathbb{R}^{m\times n}$, $\mathbf{b} \in \mathbb{R}^m$, and $\boldsymbol{\varepsilon} \in \mathbb{R}^m$ is the noise. This problem can be addressed by solving the following optimization,

$$\min_{\mathbf{x}\in\mathbb{R}^n} \ \frac{1}{2}\|\mathbf{A}\mathbf{x} - \mathbf{b}\|_q^q, \quad \text{s.t.} \ \ \mathbf{x} \in \{0,1\}^n,$$

where $\|\mathbf{x}\|_q^q = \sum_{i=1}^n |x_i|^q$ and $q > 1$. We generate $(\mathbf{A}, \mathbf{b}, \mathbf{x}^*)$ as follows. Entries of $\mathbf{A}$ are independently and identically distributed (i.i.d.) from $\mathcal{N}(0,1)$, a normal distribution with mean 0 and variance 1, and then let $\mathbf{A} = \mathbf{A}/c$, where $c = \sqrt{m}$ if $n \leqslant 10^4$ and $c = 1$ otherwise. Ground truth signal $\mathbf{x}^*$ is taken from $\{0,1\}^n$ with randomly picked $s$ indices on which entries are 1. Finally, let $\mathbf{b} = \mathbf{A}\mathbf{x}^* + \mathrm{nf} \cdot \boldsymbol{\varepsilon}$, where nf is the noise ratio and the $i$th entry of the noise is $\varepsilon_i \sim \mathcal{N}(0,1)$.

### 5.1.1 Benchmark methods

The algorithms selected for the comparison include NPGM, MEPM [39], L2ADMM [36], EMADM [18], and GUROBI. Specifically, NPGM denotes Nesterov's proximal gradient method applied to the LP relaxation of (UBIP), while EMADM is employed to solve its semidefinite relaxation. It should be emphasized that both GUROBI and EMADM are only capable of handling binary quadratic programming instances, i.e., the recovery problem with $q = 2$. Parameters for all algorithms are configured as follows. For ShaPeak, we set $\eta = 2.5$, $\sigma = (2.5, (0.6 - s/n)10^{p-3})$, $\mu_0 = (5/\sqrt{n})10^t \|\mathbf{b}^\top \mathbf{A}\|$ with $t = 4 - 2q - 10s/n$, and $k_0 = \max\{10, 2\lceil 100s/(n(p-1))\rceil\}$. In this example, pre-conditioning matrix $\mathbf{Q}^k$ is fixed by $\mathbf{Q}^k \equiv \mathbf{A}^\top \mathbf{A}$. For MEPM, the parameters are set to $(\rho, \sigma, T) = (0.01, \sqrt{10}, 10)$, and for L2ADMM, $(\alpha, \sigma, T) = (0.01, \sqrt{10}, 10)$. Both methods are terminated after at most 200 iterations or when the tolerance reaches 0.01. In addition, each requires a step-size parameter $L$, corresponding to the Lipschitz constant of the gradient, which is set to $L = \|\mathbf{A}\|_F^2/n$ for computational efficiency. For EMADM, the parameters are configured as $(\beta, \lambda_0, \delta) = (0.1, 0.001, 10^{-4})$, with the maximum number of iterations set to $10^4$ and tolerance to $10^{-4}$. All algorithms are initialized at $\mathbf{x}_0 = \mathbf{0}$ and are restricted to a maximum runtime of 600 seconds. To assess performance, we denote by $\mathbf{x}$ the solution returned by a given algorithm, and report both the recovery accuracy, defined as $\mathrm{Acc} := 1 - \|\mathbf{x} - \mathbf{x}^*\|/\|\mathbf{x}^*\|$, and the computational time in seconds.

### 5.1.2 Numerical comparison

We first demonstrate the effect of different SPFs for the proposed algorithm by selecting three types of functions: $g(x; \omega, 1, 1, 1, 1)$, $g(x; \omega, a, a, 2, 2)$, and $h(x; \omega, a, a, 2, 2)$ defined in (2.3) and (2.4). Setting $a = 2.5$ and $\omega \in \{0, 0.5, 1\}$ yields nine distinct functions in total. We fixed $(m, n, \mathrm{nf}) = (500, 1000, 0)$ while varying $q \in \{1.5, 2, 2.5\}$ and $s \in \{100, 200, \ldots, 500\}$. The median performance over 50 independent trials is reported in Table 3, where $\mathrm{SPF}_1 - \mathrm{SPF}_9$ stand for $g(x; 0, 1, 1, 1, 1)$, $g(x; 0, 2.5, 2.5, 2, 2)$, $h(x; 0, 2.5, 2.5, 2, 2)$, $g(x; 1, 1, 1, 1, 1)$, $g(x; 1, 2.5, 2.5, 2, 2)$, $h(x; 1, 2.5, 2.5, 2, 2)$, $g(x; 0.5, 1, 1, 1, 1)$, $g(x; 0.5, 2.5, 2.5, 2, 2)$, and $h(x; 0.5, 2.5, 2.5, 2, 2)$, respectively. As shown in the table, in most cases, the last two functions

$$g(x; 0.5, 2.5, 2.5, 2, 2) = \begin{cases} (2x+5)^2/8 - 25/8, & x \leqslant 1/2, \\ (2x-7)^2/8 - 25/8, & x > 1/2, \end{cases}$$

$$h(x; 0.5, 2.5, 2.5, 2, 2) = \begin{cases} 25/8 - (2x-5)^2/8, & x \leqslant 1/2, \\ 25/8 - (2x+3)^2/8, & x > 1/2, \end{cases}$$

consistently achieve the highest accuracy. Therefore, we select them in the subsequent numerical experiment, and denote the resulting algorithms as ShaPeakg and ShaPeakh.

**a) Effect of $m$.** We fix $(n, s, q, \mathrm{nf}) = (1000, 100, 2, 0)$ and vary $m \in \{250, 300, \ldots, 500\}$. For each case of $(m, n, s, q, \mathrm{nf})$, we run 20 trials and report the median results. As shown in Figure 4a, recovery accuracy generally improves with increasing $m$. When $m = 250$, only ShaPeakg and ShaPeakh achieve 100% accuracy. Once $m \geqslant 350$, all algorithms except NPGM attain 100% accuracy.

**b) Effect of $s$.** We fix $(m, n, q, \mathrm{nf}) = (500, 1000, 2, 0)$ and vary $s \in \{250, 300, \ldots, 500\}$. The median results over 20 independent trials are reported in Figure 4b. As $s$ increases, recovering the ground-

Table 3: Comparison of different SPFs.

| | $s/n$ | $\text{SPF}_1$ | $\text{SPF}_2$ | $\text{SPF}_3$ | $\text{SPF}_4$ | $\text{SPF}_5$ | $\text{SPF}_6$ | $\text{SPF}_7$ | $\text{SPF}_8$ | $\text{SPF}_9$ |
|---|---|---|---|---|---|---|---|---|---|---|
| | 0.1 | 1.00 | 1.00 | 1.00 | 1.00 | 1.00 | 1.00 | 1.00 | 1.00 | 1.00 |
| $q = 1.5$ | 0.3 | 1.00 | 1.00 | 1.00 | 1.00 | 1.00 | 1.00 | 1.00 | 1.00 | 1.00 |
| | 0.5 | 1.00 | 1.00 | 1.00 | 1.00 | 1.00 | 1.00 | 1.00 | 1.00 | 1.00 |
| | 0.1 | 1.00 | 1.00 | 1.00 | 1.00 | 1.00 | 1.00 | 1.00 | 1.00 | 1.00 |
| $q = 2.0$ | 0.3 | 1.00 | 1.00 | 1.00 | 1.00 | 1.00 | 1.00 | 1.00 | 1.00 | 1.00 |
| | 0.5 | 1.00 | 1.00 | 1.00 | 1.00 | 1.00 | 1.00 | 1.00 | 1.00 | 1.00 |
| | 0.1 | 1.00 | 1.00 | 1.00 | 1.00 | 1.00 | 1.00 | 1.00 | 1.00 | 1.00 |
| $q = 2.5$ | 0.3 | 1.00 | 1.00 | 1.00 | 1.00 | 1.00 | 1.00 | 1.00 | 1.00 | 1.00 |
| | 0.5 | 0.52 | 0.38 | 0.79 | 0.50 | 0.57 | 0.58 | 1.00 | 1.00 | 1.00 |

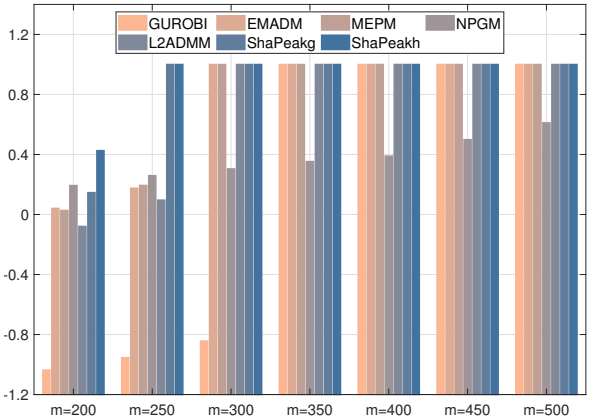


(a) Acc v.s. $m$

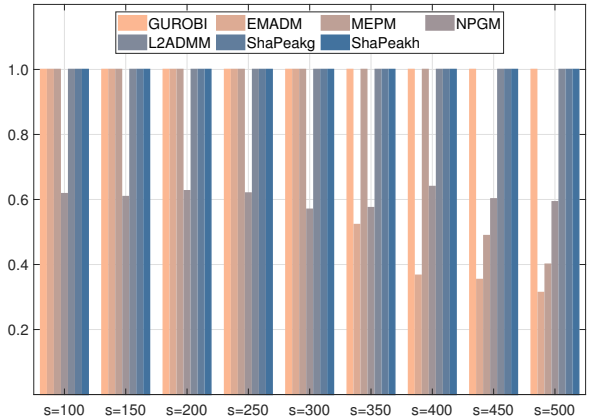


(b) Acc v.s. $s$

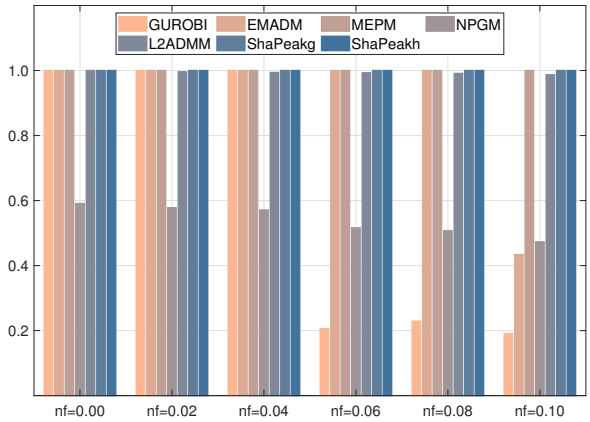


(c) Acc v.s. nf

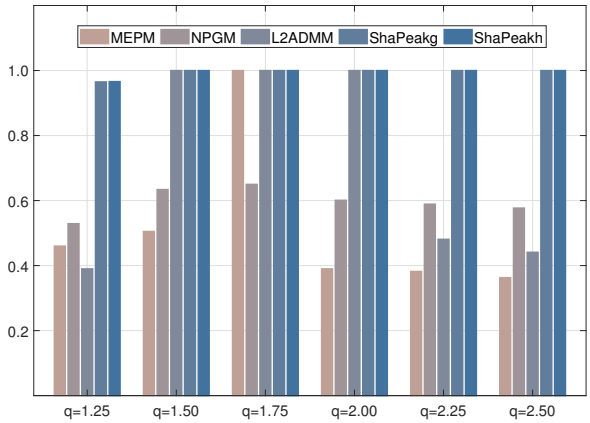


(d) Acc v.s. $q$

Figure 4: Results on recovery problems.

truth signal becomes progressively more challenging. Across all settings, ShaPeakg, ShaPeakh, L2ADMM, and GUROBI can achieve exact recovery due to the achievement of 100% accuracy.

**c) Effect of** nf**.** We fix $(m, n, s, q) = (500, 1000, 300, 2)$ but increase nf over range $\{0, 0.02, \ldots, 0.1\}$. The median results over 20 trials are reported in Figure 4c. It can be observed that ShaPeakg, ShaPeakh, MEPM, and L2ADMM are robust to noise, whereas GUROBI (within 600 seconds) and EMADM fail to recover the signal when nf $\geqslant 0.06$ and nf $= 0.1$, respectively.

Table 4: Effect of higher dimensions, where A1-A5 stand for ShaPeakg, ShaPeakh, MEPM, L2ADMM, and LP, respectively.

| $n$ | nf | Acc | | | | | Time | | | | |
|---|---|---|---|---|---|---|---|---|---|---|---|
| | | A1 | A2 | A3 | A4 | A5 | A1 | A2 | A3 | A4 | A5 |
| | | | | | | $q = 1.5$ | | | | | |
| $10^4$ | 0.0 | 1.000 | 1.000 | 1.000 | 0.992 | 0.614 | 0.219 | 0.212 | 24.06 | 38.75 | 3.118 |
| $10^4$ | 0.1 | 1.000 | 1.000 | 1.000 | 0.991 | 0.594 | 0.214 | 0.189 | 29.67 | 50.55 | 3.267 |
| $10^5$ | 0.0 | 1.000 | 1.000 | 1.000 | 1.000 | -0.116 | 12.70 | 12.61 | 910.6 | 1197.4 | 38.53 |
| $10^5$ | 0.1 | 1.000 | 1.000 | 1.000 | 0.996 | -0.083 | 43.76 | 43.32 | 1055.1 | 1430.7 | 45.20 |
| $10^6$ | 0.0 | 1.000 | 1.000 | -3.383 | -3.157 | -1.778 | 49.76 | 53.45 | 3283.4 | 3600.0 | 119.2 |
| $10^6$ | 0.1 | 1.000 | 1.000 | -3.363 | -2.879 | -1.785 | 121.3 | 125.7 | 3600.0 | 3600.0 | 147.4 |
| | | | | | | $q = 2$ | | | | | |
| $10^4$ | 0.0 | 1.000 | 1.000 | 1.000 | 1.000 | 0.658 | 0.224 | 0.210 | 18.38 | 26.94 | 2.992 |
| $10^4$ | 0.1 | 1.000 | 1.000 | 1.000 | 0.996 | 0.647 | 0.254 | 0.245 | 21.16 | 32.55 | 3.170 |
| $10^5$ | 0.0 | 1.000 | 1.000 | -5.581 | -5.481 | -4.573 | 8.986 | 8.933 | 1248.3 | 1253.4 | 37.23 |
| $10^5$ | 0.1 | 1.000 | 1.000 | -5.566 | -4.208 | -4.574 | 10.28 | 10.05 | 1565.6 | 1869.3 | 44.55 |
| $10^6$ | 0.0 | 1.000 | 1.000 | -5.565 | -4.118 | -4.562 | 40.41 | 41.22 | 3198.2 | 3415.9 | 108.3 |
| $10^6$ | 0.1 | 1.000 | 1.000 | -5.577 | -5.469 | -4.562 | 128.3 | 127.6 | 3600.0 | 3600.0 | 136.1 |
| | | | | | | $q = 2.5$ | | | | | |
| $10^4$ | 0.0 | 1.000 | 1.000 | -5.837 | -5.835 | -5.705 | 0.517 | 0.507 | 38.99 | 39.06 | 3.172 |
| $10^4$ | 0.1 | 1.000 | 1.000 | -5.865 | -5.456 | -5.563 | 0.497 | 0.496 | 54.44 | 67.14 | 3.341 |
| $10^5$ | 0.0 | 1.000 | 1.000 | -5.843 | -5.844 | -5.808 | 22.57 | 23.54 | 1300.1 | 1281.5 | 8.623 |
| $10^5$ | 0.1 | 1.000 | 1.000 | -5.834 | -5.293 | -5.792 | 24.59 | 24.80 | 1536.5 | 2214.1 | 45.73 |
| $10^6$ | 0.0 | 1.000 | 1.000 | -5.789 | -5.822 | -5.706 | 49.24 | 50.09 | 3556.0 | 3600.0 | 121.9 |
| $10^6$ | 0.1 | 0.982 | 0.982 | -5.801 | -5.793 | -5.710 | 65.04 | 67.45 | 3600.0 | 3600.0 | 149.9 |

**d) Effect of $q$.** We fix $(m, n, s, \text{nf}) = (500, 1000, 500, 0)$ but increase $q$ over range $\{1.25, 1.5, \ldots, 2.5\}$. The median results over 20 trials are reported in Figure 4d. As mentioned earlier, GUROBI and EMADM cannot handle non-quadratic cases (namely, $q \neq 2$) and are therefore excluded from this experiment. Again, ShaPeakg and Shapeakh maintain the highest accuracy for all cases.

**e) Effect of higher dimensions.** In this experiment, we exclude GUROBI and EMADM for the comparison due to their dramatically increased computational time when $n \geqslant 10^4$. By fixing $(m, s) = (0.5n, 0.01n)$, we choose $n \in \{10^4, 10^5, 10^6\}$ and $\text{nf} \in \{0, 0.5\}$. Moreover, sparse matrices $\mathbf{A}$ with $10^8$ nonzero entries are used when $n \geqslant 10^5$, resulting in density $10^9/(5n^2)$. Table 4 reports the median results over 10 independent runs. For each $(n, \text{nf})$, two ShaPeak algorithms achieve the highest accuracy and the shortest computation time, demonstrating superior performance.

### 5.2 MIMO detection

We consider two types of MIMO detection problems: classical and one-bit MIMO detection. The former involves a quadratic objective function, whereas the latter features a non-quadratic one.

### 5.2.1 Classical MIMO detection

The task of the classical MIMO detection is to recover a signal $\mathbf{w}^*$ from a linear model, $\mathbf{y} = \mathbf{H}\mathbf{w}^* + \boldsymbol{\varepsilon}$, where $\mathbf{H} \in \mathbb{C}^{m \times n/2}$ is the channel matrix, $\mathbf{y} \in \mathbb{C}^m$ is the received signal, and $\boldsymbol{\varepsilon} \in \mathbb{C}^m$ is the Gaussian noise whose entries are i.i.d. from $\mathcal{N}(0, \varrho^2)$. Let ground truth signal $\mathbf{w}^* \in \Omega := \{\mathbf{w} \in \mathbb{C}^{n/2} : \mathrm{Re}(\mathbf{w}) \in \{0,1\}^{n/2}, \mathrm{Im}(\mathbf{w}) \in \{0,1\}^{n/2}\}$, where $\mathrm{Re}(\mathbf{w})$ and $\mathrm{Im}(\mathbf{w})$ represent the real and imagery part of $\mathbf{w}$. The classical MIMO detection can be addressed by maximizing the likelihood as follows,

$$\min_{\mathbf{x} \in \mathbb{R}^n} \quad \frac{1}{2}\|\mathbf{A}\mathbf{x} - \mathbf{b}\|^2, \quad \text{s.t.} \;\; \mathbf{x} \in \{0,1\}^n,$$

where

$$\mathbf{A} := \begin{bmatrix} \mathrm{Re}(\mathbf{H}) & -\mathrm{Im}(\mathbf{H}) \\ \mathrm{Im}(\mathbf{H}) & \mathrm{Re}(\mathbf{H}) \end{bmatrix}, \qquad \mathbf{b} := \begin{bmatrix} \mathrm{Re}(\mathbf{y}) \\ \mathrm{Im}(\mathbf{y}) \end{bmatrix}, \qquad \mathbf{x} := \begin{bmatrix} \mathrm{Re}(\mathbf{w}) \\ \mathrm{Im}(\mathbf{w}) \end{bmatrix}.$$

We consider two types of channel matrices $\mathbf{H}$. The first corresponds to the i.i.d. Gaussian channel case, where the entries of $\mathrm{Re}(\mathbf{H})$ and $\mathrm{Im}(\mathbf{H})$ are generated in the same manner as the entries of $\mathbf{A}$ in Section 5.1. The second corresponds to the correlated MIMO channel case, following a similar approach to [19, 28]. Specifically, let $\widetilde{\mathbf{H}}$ be an element-wise i.i.d. circularly symmetric complex Gaussian matrix with zero mean and unit variance. Let $\mathbf{R}$ and $\mathbf{T}$ denote the spatial correlation matrices at the receiver and transmitter, respectively, with each entry $R_{ij}$ of $\mathbf{R}$ defined as

$$R_{ij} = \begin{cases} r^{i-j}, & \text{if } i \leqslant j, \\ R_{ij}^*, & \text{if } i > j, \end{cases}$$

where $|r| \leqslant 1$. The matrix $\mathbf{T}$ is generated in the same way. By performing Cholesky-like decompositions $\mathbf{R} = \mathbf{P}\mathbf{P}^*$ and $\mathbf{T} = \mathbf{Q}\mathbf{Q}^*$, the correlated channel matrix is constructed as $\mathbf{H} = \mathbf{P}\widetilde{\mathbf{H}}\mathbf{Q}$. In the sequel, we set $r = 0.2$ and $\mathbf{R} = \mathbf{T}$. Transmit signal $\mathbf{w}^*$ is generated element-wise from a uniform distribution over the quaternary phase-shift keying constellation; see [28] for more details. The signal-to-noise ratio (SNR), which is used to determine the noise variance $\varrho^2$, is defined as

$$\mathrm{SNR} = \mathbb{E}\,\|\mathbf{H}\mathbf{w}^*\|^2 / \mathbb{E}\,\|\boldsymbol{\varepsilon}\|^2 .$$

**a) Benchmark methods.** We select MEPM, L2ADMM, and HOTML [28] for the comparison and also report the results directly calculated by two detectors: zero-forcing detector (ZF) and minimum-mean-square-error (MMSE) decision-feedback detector. Moreover, we assume no inter-signal interference and establish a lower bound (LB) for the problem, as described in [28]. Parameters for all algorithms are given as follows. For ShaPeak, we set $(\eta, \sigma, k_0) = (3, 32/\log_{10}(N), 10)$ and $\mu_0 = \sqrt{N}10^{-4}\|\mathbf{y}^\top \mathbf{H}\|_\infty$. Again, pre-conditioning matrix is predefined as $\mathbf{Q}^k \equiv \mathbf{A}^\top \mathbf{A}$. The settings for MEPM and L2ADMM are also the same as those in Section 5.1. For HOTML, we set $\sigma_0 = 0.5$ and $\lambda_0 = 0.001$. It terminates when either the number of iterations $k > 200$ or $\|\lambda_k - \lambda_{k-1}\| \leq 10^{-4}$ is satisfied. Once again, for fairness, all algorithms are initialized with $\mathbf{x}^0 = \mathbf{0}$. We evaluate performance using the bit error rate (BER) defined by

$$\mathrm{BER} = \frac{|\{i \in [n] : x_i \neq x_i^*\}|}{n},$$

where $|\Omega|$ is the cardinality of set $\Omega$. Note that a lower BER indicates more accurate recovery.

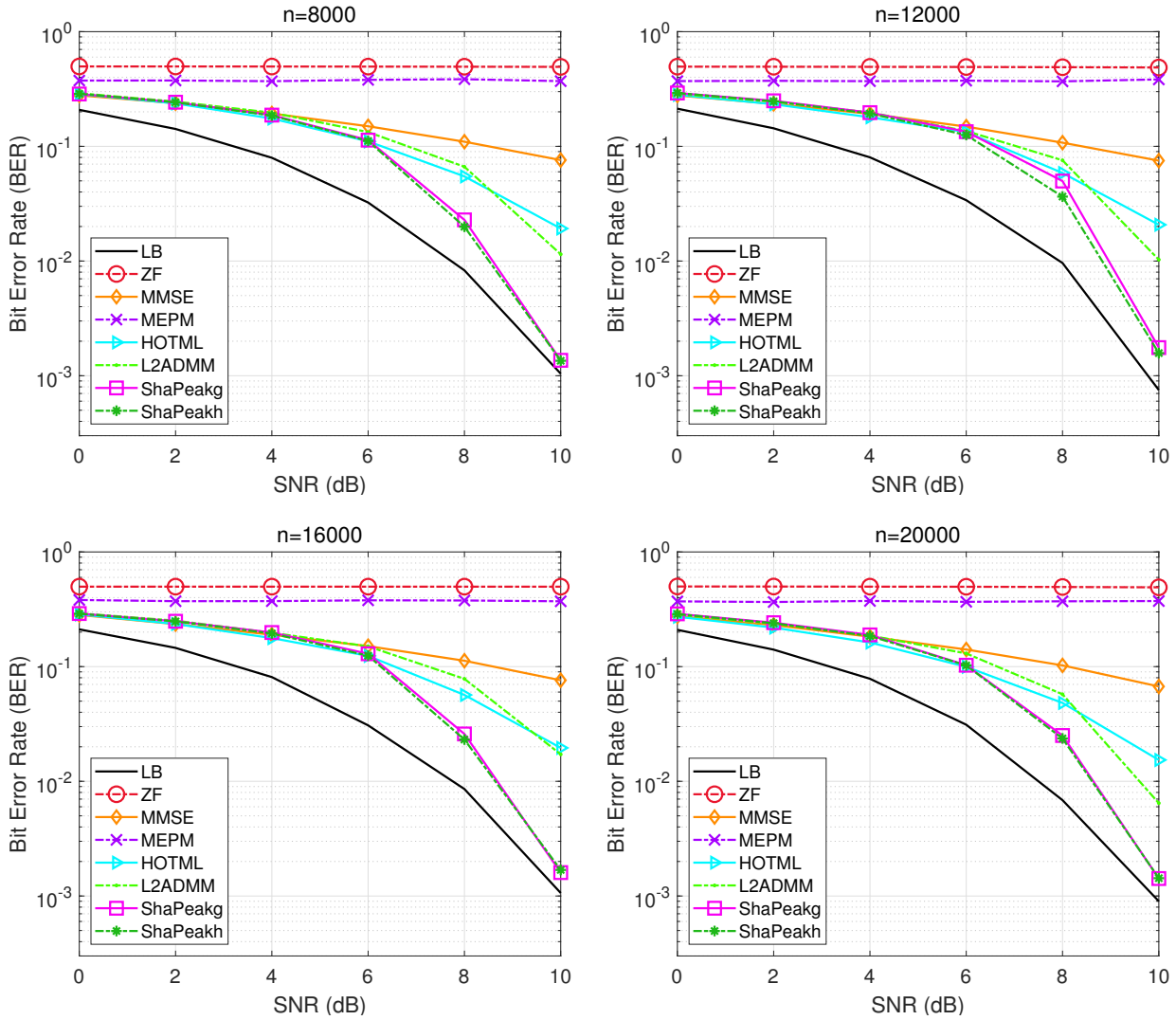


Figure 5: Results on classical MIMO detection problems for i.i.d channels.

**b) Numerical comparison.** We consider the case of critically determined channels (i.e., $m = n/2$) with $n \in \{8000, 12000, 16000, 20000\}$. Figures 5 and 6 present the numerical results for the i.i.d. and correlated channels, respectively. All reported results are averaged over 20 independent trials. For the i.i.d. channel case, ShaPeak achieves the best BER performance, followed by L2ADMM and HOTML, while ZF performs the worst. In the correlated channel setting, ShaPeak continues to attain the lowest BER across most SNR levels, followed by HOTML, whereas L2ADMM fails under this configuration. The corresponding computational time is reported in Table 5. ShaPeak demonstrates a significant advantage in all scenarios. For example, under the i.i.d. channel with SNR $= 10$ and $n = 20000$, ShaPeakg and ShaPeakh complete in 6.045 and 5.934 seconds, respectively, while the other three methods each require over 200 seconds.

### 5.2.2 One-bit MIMO detection

The task of one-bit MIMO detection [28] is to detect $\mathbf{z} \in \{-1, 1\}^n$ from the following model,

$$\mathbf{y} = \mathrm{sgn}(\mathbf{H}\mathbf{z} + \mathbf{v}), \tag{5.1}$$

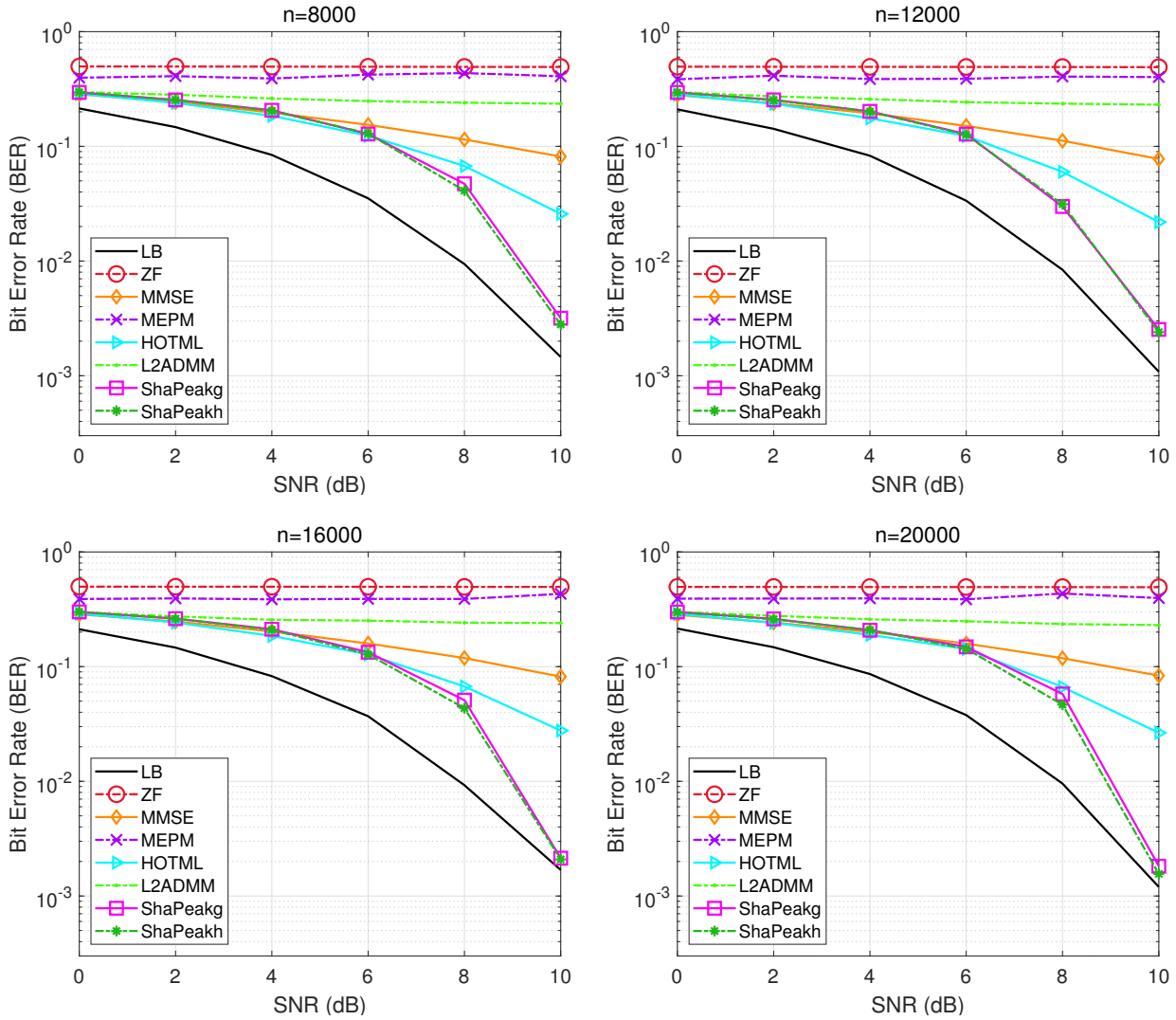


Figure 6: Results on classical MIMO detection problems for correlated channels.

where $\mathrm{sgn}(\cdot)$ denotes the element-wise sign function, $\mathbf{H} \in \mathbb{R}^{m\times n}$ is a system matrix, and $\mathbf{v} \in \mathbb{R}^m$ is the Gaussian noise whose entries are i.i.d. variable from $\mathcal{N}(0, \varrho^2)$. Under model (5.1), the maximum-likelihood detector takes the form

$$\min_{\mathbf{z}\in\mathbb{R}^n} \quad -\sum_{i=1}^{m} \log \Phi\left((y_i/\varrho)\langle \mathbf{h}_i, \mathbf{z}\rangle\right), \quad \text{s.t.} \;\; \mathbf{z} \in \{-1, 1\}^n, \tag{5.2}$$

where $\Phi(t) = \int_{-\infty}^{t} \frac{1}{\sqrt{2\pi}} e^{-\tau^2/2} d\tau$ and $\mathbf{h}_i$ denotes the $i$ th row of $\mathbf{H}$. By substituting $\mathbf{x} = (\mathbf{z}+1)/2$, one can easily rewrite (5.2) in the form of (UBIP).

**a) Benchmark methods.** The methods selected for the comparison include ZF, MEPM, L2ADMM, and HOTML. Parameters are set as follows. For ShaPeak, we set $(\eta, \sigma, k_0) = (2.25+0.25r, 0.001N, 10)$ and $\mu_0 = (1+4r)10^{-3}\log_{10}(N)\|\mathbf{y}^\top \mathbf{H}\|_\infty$, where $r = 0$ if $N < 5000$ and $r = 1$ otherwise. Preconditioning matrix is chosen as $\mathbf{Q}^k = \mathbf{H}^\top \mathrm{Diag}(\mathbf{y}\odot\mathbf{y})\mathbf{H}/\varrho^2$ serving as an approximation of the Hessian of $f$, where $\mathrm{Diag}(\mathbf{y})$ denotes the diagonal matrix formed by $\mathbf{y}$ and $\mathbf{x}\odot\mathbf{y}$ is the Hadamard product of $\mathbf{x}$ and $\mathbf{y}$. For MEPM and L2ADMM, we set $L = \|\mathbf{H}\|_F^2/n$. HOTML adopts the same parameter settings as in the classical MIMO case. Its maximum number of iterations is set to 300.

Table 5: Average CPU time (in seconds) for classical MIMO detection problems, where A1-A5 stand for ShaPeakg, ShaPeakh, MEPM, L2ADMM, and HOTML, respectively.

| | I.I.D channels | | | | | Correlated channels | | | | |
|---|---|---|---|---|---|---|---|---|---|---|
| SNR | A1 | A2 | A3 | A4 | A5 | A1 | A2 | A3 | A4 | A5 |
| | | | | | $n = 8000$ | | | | | |
| 0 | 1.345 | 1.227 | 28.06 | 37.60 | 28.25 | 1.128 | 1.122 | 28.42 | 36.60 | 28.12 |
| 2 | 1.441 | 1.393 | 28.09 | 38.18 | 26.08 | 1.185 | 1.104 | 27.70 | 36.72 | 25.85 |
| 4 | 1.438 | 1.463 | 28.17 | 38.22 | 26.12 | 1.264 | 1.039 | 28.42 | 34.68 | 25.86 |
| 6 | 1.536 | 1.266 | 28.04 | 38.38 | 26.18 | 1.268 | 1.174 | 27.29 | 34.46 | 25.87 |
| 8 | 1.406 | 1.355 | 27.94 | 38.47 | 26.40 | 1.245 | 1.219 | 27.99 | 34.39 | 25.85 |
| 10 | 1.129 | 1.123 | 27.98 | 38.38 | 26.12 | 0.930 | 0.916 | 27.93 | 34.44 | 25.84 |
| | | | | | $n = 12000$ | | | | | |
| 0 | 2.324 | 2.051 | 67.15 | 88.25 | 103.8 | 2.901 | 2.844 | 68.21 | 93.14 | 104.8 |
| 2 | 2.669 | 2.190 | 68.48 | 92.39 | 103.4 | 2.903 | 2.844 | 70.58 | 91.65 | 101.5 |
| 4 | 2.695 | 2.373 | 68.74 | 92.60 | 103.3 | 2.910 | 2.854 | 70.24 | 86.82 | 101.5 |
| 6 | 2.298 | 2.069 | 68.24 | 92.21 | 103.4 | 2.867 | 2.864 | 69.64 | 84.01 | 101.5 |
| 8 | 2.169 | 2.014 | 68.21 | 92.66 | 103.8 | 2.891 | 2.864 | 70.35 | 84.27 | 101.5 |
| 10 | 1.767 | 1.728 | 68.33 | 92.45 | 103.7 | 2.059 | 2.026 | 68.53 | 85.37 | 101.6 |
| | | | | | $n = 16000$ | | | | | |
| 0 | 5.668 | 5.625 | 133.9 | 181.5 | 254.5 | 5.652 | 5.614 | 128.4 | 177.5 | 256.9 |
| 2 | 5.661 | 5.619 | 134.1 | 180.7 | 251.6 | 5.641 | 5.612 | 131.9 | 177.5 | 261.9 |
| 4 | 5.643 | 5.554 | 134.2 | 180.9 | 251.3 | 5.585 | 5.558 | 132.4 | 157.5 | 261.9 |
| 6 | 5.675 | 5.609 | 134.1 | 181.8 | 251.3 | 5.655 | 5.574 | 129.9 | 157.3 | 261.8 |
| 8 | 5.668 | 5.609 | 134.5 | 182.5 | 251.7 | 5.754 | 5.551 | 130.7 | 156.9 | 262.0 |
| 10 | 4.047 | 3.988 | 133.0 | 179.9 | 253.1 | 3.992 | 3.960 | 127.6 | 159.7 | 261.8 |
| | | | | | $n = 20000$ | | | | | |
| 0 | 8.474 | 8.421 | 204.8 | 254.3 | 493.9 | 8.492 | 9.915 | 199.7 | 268.5 | 495.6 |
| 2 | 8.706 | 8.570 | 204.4 | 274.7 | 496.4 | 8.349 | 9.326 | 205.4 | 290.1 | 509.4 |
| 4 | 8.574 | 8.476 | 204.2 | 275.3 | 496.7 | 8.502 | 8.946 | 204.6 | 263.0 | 509.6 |
| 6 | 8.610 | 8.435 | 205.0 | 275.3 | 496.2 | 8.431 | 8.203 | 202.5 | 246.4 | 498.9 |
| 8 | 8.507 | 8.435 | 204.4 | 277.8 | 496.5 | 9.344 | 8.581 | 206.2 | 244.0 | 509.1 |
| 10 | 6.045 | 5.934 | 204.8 | 276.6 | 497.0 | 5.883 | 5.789 | 206.2 | 258.9 | 509.1 |

**b) Numerical comparison.** We first evaluate the performance of all algorithms under different values of $m/n$. Specifically, we fix SNR $= 15$, set $n \in \{500, 1000\}$, and vary $m/n \in \{1, 1.5, \ldots, 3\}$. Figure 7 reports the average results over 20 independent trials. As expected, a larger ratio results in lower BER, indicating easier recovery. It is evident that ShaPeakg and ShaPeakh consistently achieve the lowest BER across all cases.

Next, we fix $m/n = 2$, choose $n \in \{500, 1000\}$, and vary SNR $\in \{0, 5, \ldots, 20\}$. The average results over 20 runs are presented in Figure 8. When SNR $\leqslant 10$, none of the algorithms achieve satisfactory BER performance, indicating failure in signal recovery. As SNR increases, ShaPeak begins to

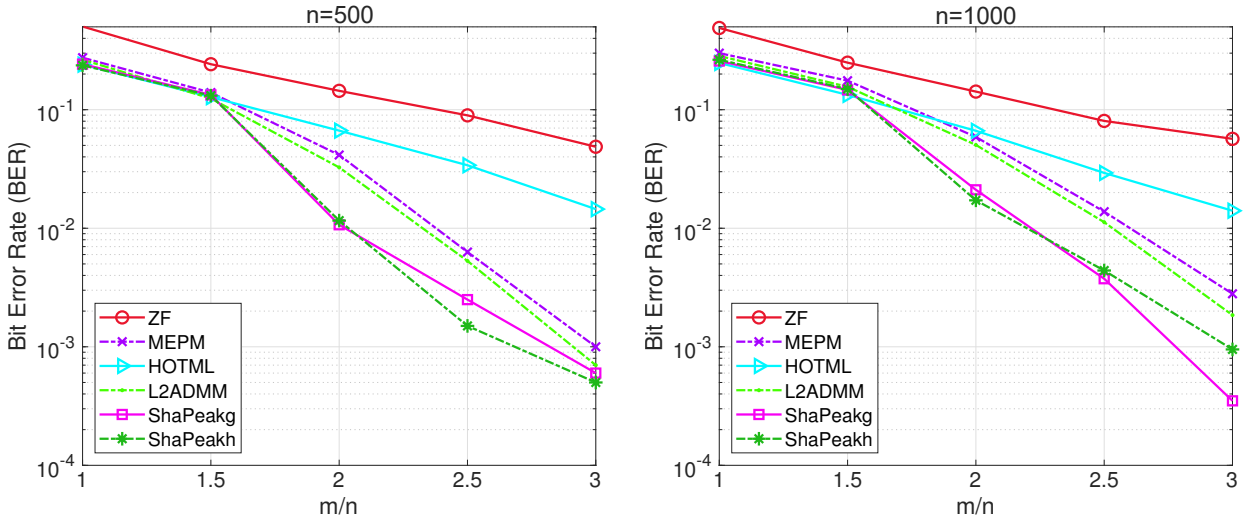


Figure 7: Effect of $m/n$ for one-bit MIMO detection problems.

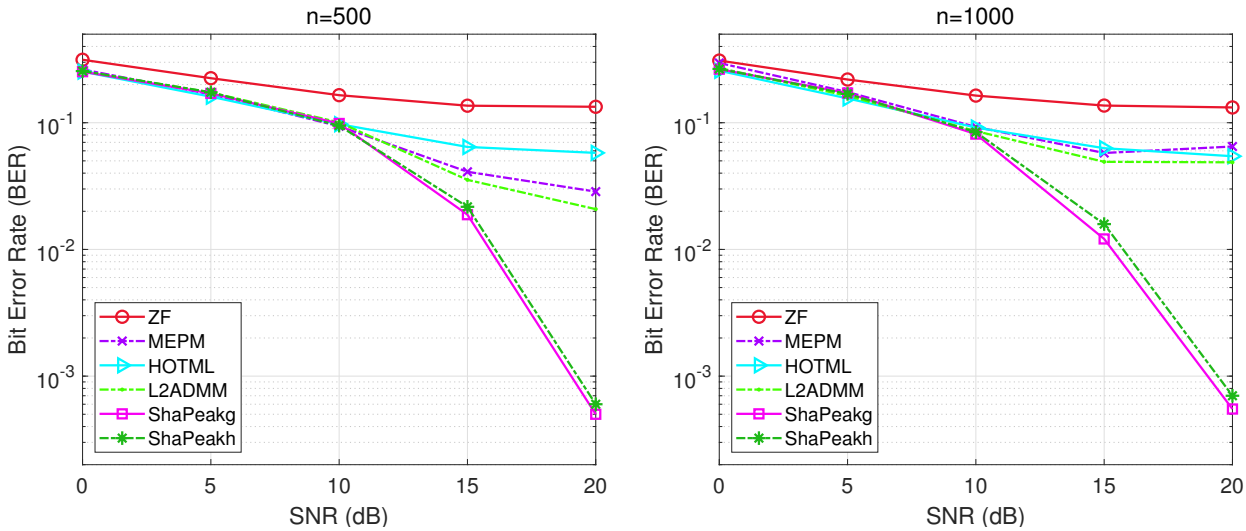


Figure 8: Effect of SNR for one-bit MIMO detection problems.

outperform the other algorithms, with its advantage becoming more pronounced at higher SNR levels. Regarding computational efficiency, we consider a slightly high dimension $n = 5000$. As reported in Table 6, ShaPeak demonstrates significantly lower runtime. For instance, in the case of SNR $= 20$, ShaPeakg and ShaPeakh complete in 10.87 and 10.86 seconds, respectively, while L2ADMM requires nearly 200 seconds.

### 5.3 QUBO

The QUBO problem takes the following form,

$$\min_{\mathbf{x}\in\mathbb{R}^n} \ \frac{1}{2}\langle \mathbf{x}, \mathbf{Q}\mathbf{x}\rangle, \quad \text{s.t.} \ \ \mathbf{x} \in \{0,1\}^n,$$

where $\mathbf{Q} \in \mathbb{R}^n$ is a symmetric matrix. Following the approach in [6], we generate the matrix $\mathbf{Q}$ as follows. For $n < 10^4$, $\mathbf{Q}$ is a dense matrix with a density of 0.8, and its nonzero entries are drawn independently from the uniform distribution over interval $[10, 100]$. For large-scale problems with $n \geqslant 10^4$, $\mathbf{Q}$ is generated as a sparse matrix with a density of 0.005. The algorithms benchmarked in

Table 6: Average BER and CPU time (in seconds) for higher dimensional instances, where A1-A6 stand for ShaPeakg, ShaPeakh, MEPM, L2ADMM, HOTML, and ZF, respectively.

| | BER | | | | | | Time | | | | |
|---|---|---|---|---|---|---|---|---|---|---|---|
| SNR | A1 | A2 | A3 | A4 | A5 | A6 | A1 | A2 | A3 | A4 | A5 |
| 0 | 0.273 | 0.271 | 0.474 | 0.441 | 0.257 | 0.312 | 2.044 | 1.949 | 142.9 | 188.4 | 9.978 |
| 5 | 0.171 | 0.173 | 0.340 | 0.289 | 0.157 | 0.224 | 4.856 | 4.317 | 143.4 | 196.8 | 12.36 |
| 10 | 0.092 | 0.088 | 0.219 | 0.177 | 0.095 | 0.167 | 6.825 | 6.744 | 139.8 | 196.3 | 20.21 |
| 15 | 0.015 | 0.016 | 0.164 | 0.136 | 0.068 | 0.144 | 9.245 | 8.937 | 144.0 | 195.7 | 20.35 |
| 20 | 0.001 | 0.001 | 0.154 | 0.138 | 0.064 | 0.134 | 10.87 | 10.86 | 143.0 | 197.2 | 20.49 |

Table 7: Gap for low-dimensional instances

| | ShaPeakg | | ShaPeakh | | MEPM | | L2ADMM | | GUROBI | | SDPNAL+ | |
|---|---|---|---|---|---|---|---|---|---|---|---|---|
| $n$ | best | mean | best | mean | best | mean | best | mean | best | mean | best | mean |
| 1000 | 0.19 | 0.58 | 0.18 | 0.55 | 1.54 | 4.64 | 0.81 | 2.62 | 0.00 | 0.00 | 3.86 | 5.27 |
| 3000 | 0.46 | 0.59 | 0.46 | 0.59 | 3.64 | 4.08 | 3.27 | 3.64 | 0.00 | 0.00 | 5.01 | 6.02 |
| 5000 | 0.39 | 0.52 | 0.41 | 0.55 | 4.17 | 4.54 | 3.69 | 4.10 | 0.00 | 0.00 | 8.41 | 10.0 |
| 7000 | 0.28 | 0.41 | 0.24 | 0.39 | 4.85 | 5.11 | 4.35 | 4.62 | 0.00 | 0.00 | 42.5 | 47.5 |
| 10000 | 0.24 | 0.37 | 0.21 | 0.37 | 5.32 | 5.81 | 4.84 | 5.47 | 0.00 | 0.00 | 64.3 | 67.9 |

Table 8: Time (in seconds) for low-dimensional instances

| $n$ | ShaPeakg | ShaPeakh | MEPM | L2ADMM | GUROBI | SDPNAL+ |
|---|---|---|---|---|---|---|
| 1000 | 0.062 | 0.053 | 0.337 | 0.447 | 600.0 | 176.6 |
| 3000 | 0.299 | 0.271 | 2.956 | 3.605 | 600.0 | 600.0 |
| 5000 | 1.296 | 1.224 | 21.65 | 26.38 | 600.0 | 600.0 |
| 7000 | 2.748 | 2.696 | 47.50 | 58.01 | 600.0 | 600.0 |
| 10000 | 5.854 | 5.934 | 109.5 | 130.6 | 600.0 | 600.0 |

this experiment include MEPM, L2ADMM, GUROBI, and SDPNAL+ [30]. The hyperparameters are given as follows. For ShaPeak, we set $(\eta, \sigma, k_0) = (2.1, 0.01, 10)$ and $\mu_0 = (10^{-5}/2)\|\mathbf{Q}\|_F$. Since $\mathbf{Q}$ may not be positive semi-definite, we choose $\mathbf{Q}^k \equiv \mathbf{0}$ rather than $\mathbf{Q}^k \equiv \mathbf{Q}$. For MEPM and L2ADMM, we set $L = \|\mathbf{Q}\|_F^2/n$, while other parameters remain consistent with those used in previous experiments. Default settings are adopted for GUROBI and SDPNAL+. To evaluate performance, we compute the relative optimality gap defined as follows, where 'obj' denotes the objective value obtained by a specific algorithm, and 'lowest' refers to the lowest objective value achieved among all compared methods.

$$\text{Gap} = \frac{|\text{obj} - \text{lowest}|}{|\text{lowest}|} \times 100\%,$$

Tables 7 and 8 report results over 20 independent runs for small-scale problems, where 'best' and 'mean' denote the best and average Gap. In all scenarios, GUROBI achieves the smallest gap, while ShaPeakg and ShaPeakh rank next and exhibit a significant speed advantage. We then extend the comparison to higher dimensional settings, $n = 80000$ and $n = 10^5$, excluding GUROBI

Table 9: Gap and time (in seconds) for higher dimensional instances

| | | ShaPeakg | | | ShaPeakh | | | MEPM | | | L2ADMM | | |
|---|---|---|---|---|---|---|---|---|---|---|---|---|---|
| $n$ | case | best | mean | time | best | mean | time | best | mean | time | best | mean | time |
| | 1 | 0.01 | 0.02 | 33.59 | 0.00 | 0.00 | 33.29 | 1.55 | 1.59 | 601.1 | 1.30 | 1.31 | 778.7 |
| | 2 | 0.00 | 0.01 | 32.72 | 0.00 | 0.01 | 33.48 | 1.59 | 1.62 | 615.8 | 1.32 | 1.34 | 783.2 |
| 8e4 | 3 | 0.00 | 0.02 | 32.65 | 0.00 | 0.00 | 32.70 | 1.56 | 1.58 | 620.5 | 1.28 | 1.31 | 770.7 |
| | 4 | 0.00 | 0.01 | 33.07 | 0.00 | 0.00 | 33.64 | 1.59 | 1.60 | 615.6 | 1.30 | 1.32 | 786.3 |
| | 5 | 0.00 | 0.01 | 32.98 | 0.00 | 0.00 | 32.91 | 1.60 | 1.61 | 630.9 | 1.33 | 1.35 | 793.9 |
| | 1 | 0.00 | 0.01 | 51.73 | 0.00 | 0.00 | 50.84 | 1.69 | 1.72 | 993.6 | 1.41 | 1.43 | 1253.1 |
| | 2 | 0.01 | 0.02 | 52.19 | 0.00 | 0.00 | 51.94 | 1.72 | 1.76 | 1011.4 | 1.44 | 1.47 | 1266.1 |
| 1e5 | 3 | 0.00 | 0.01 | 52.09 | 0.00 | 0.00 | 51.53 | 1.73 | 1.75 | 998.8 | 1.45 | 1.46 | 1254.0 |
| | 4 | 0.00 | 0.01 | 51.84 | 0.00 | 0.00 | 51.33 | 1.71 | 1.77 | 1000.2 | 1.41 | 1.47 | 1258.0 |
| | 5 | 0.00 | 0.01 | 52.31 | 0.00 | 0.00 | 50.98 | 1.64 | 1.70 | 1001.4 | 1.36 | 1.41 | 1250.9 |

and SDPNAL+ due to excessive computational time. As shown in Table 9, where case 1 - case 5 correspond to 5 different proportions $\{0.4995, 0.4999, 0.49995, 0.49999, 0.5\}$ of negative elements in matrix $\mathbf{Q}$, ShaPeakg and ShaPeakh achieve lower objective values with faster computational speed than MEPM and L2ADMM. For instance, in case 5 and $n = 10^5$, ShaPeakg and ShaPeakh consume 52.31 and 50.98 seconds, compared with 1001.4 and 1250.9 seconds for MEPM and L2ADMM.

## 6 Conclusion

The proposed sharp-peak functions reformulate binary integer programming problems into constrained optimization problems, allowing continuous optimization techniques to address inherently discrete challenges. This class of functions not only leads to a new exact penalty theorem but also enhances the algorithm's performance theoretically and numerically. Therefore, further exploration of sharp-peak functions for solving binary integer programs with additional constraints is a promising direction for future research.

## References


[1] M. F. Anjos and J. B. Lasserre. *Handbook on semidefinite, conic and polynomial optimization*, volume 166. Springer Science & Business Media, 2011.

[2] E. Baş. Binary aquila optimizer for 0–1 knapsack problems. *Engineering Applications of Artificial Intelligence*, 118:105592, 2023.

[3] C. Buchheim, M. Montenegro, and A. Wiegele. SDP-based branch-and-bound for non-convex quadratic integer optimization. *Journal of Global Optimization*, 73:485–514, 2019.

[4] C. Buchheim and A. Wiegele. Semidefinite relaxations for non-convex quadratic mixed-integer programming. *Mathematical Programming*, 141:435–452, 2013.

[5] S. Burer, R. D. Monteiro, and Y. Zhang. Rank-two relaxation heuristics for max-cut and other binary quadratic programs. *SIAM Journal on Optimization*, 12(2):503–521, 2002.

[6] C. Chen, R. Chen, T. Li, R. Ao, and Z. Wen. Monte carlo policy gradient method for binary optimization, 2023.

[7] T. Cour and J. Shi. Solving markov random fields with spectral relaxation. In *Artificial Intelligence and Statistics*, pages 75–82. PMLR, 2007.

[8] M. De Santis and F. Rinaldi. Continuous reformulations for zero–one programming problems. *Journal of Optimization Theory and Applications*, 153:75–84, 2012.

[9] M. Esmaeilpour, P. Cardinal, and A. L. Koerich. A robust approach for securing audio classification against adversarial attacks. *IEEE Transactions on Information Forensics and Security*, 15:2147–2159, 2019.

[10] M. R. Garey and D. S. Johnson. *Computers and intractability*, volume 29. wh freeman New York, 2002.

[11] C. Helmberg and F. Rendl. A spectral bundle method for semidefinite programming. *SIAM Journal on Optimization*, 10(3):673–696, 2000.

[12] C.-J. Hsieh, N. Natarajan, and I. Dhillon. PU learning for matrix completion. In *International Conference on Machine Learning*, pages 2445–2453. PMLR, 2015.

[13] Q. Huang, Y. Chen, and L. Guibas. Scalable semidefinite relaxation for maximum a posterior estimation. In *International Conference on Machine Learning*, pages 64–72. PMLR, 2014.

[14] T. Joachims et al. Transductive inference for text classification using support vector machines. In *International Conference on Machine Learning*, volume 99, pages 200–209, 1999.

[15] G. Kochenberger, J.-K. Hao, F. Glover, M. Lewis, Z. Lü, H. Wang, and Y. Wang. The unconstrained binary quadratic programming problem: A survey. *Journal of Combinatorial Optimization*, 28:58–81, 2014.

[16] N. Komodakis and G. Tziritas. Approximate labeling via graph cuts based on linear programming. *IEEE Transactions on Pattern Analysis and Machine Intelligence*, 29(8):1436–1453, 2007.

[17] J. B. Lasserre. A max-cut formulation of 0/1 programs. *Operations Research Letters*, 44(2):158–164, 2016.

[18] H. Liu, K. Deng, H. Liu, and Z. Wen. An entropy-regularized ADMM for binary quadratic programming. *Journal of Global Optimization*, 87(2):447–479, 2023.

[19] S. L. Loyka. Channel capacity of MIMO architecture using the exponential correlation matrix. *IEEE Communications letters*, 5(9):369–371, 2001.

[20] R. Merkle and M. Hellman. Hiding information and signatures in trapdoor knapsacks. *IEEE Transactions on Information Theory*, 24(5):525–530, 1978.

[21] J. J. Moré and D. C. Sorensen. Computing a trust region step. *SIAM Journal on Scientific and Statistical Computing*, 4(3):553–572, 1983.

[22] W. Murray and K.-M. Ng. An algorithm for nonlinear optimization problems with binary variables. *Computational Optimization and Applications*, 47(2):257–288, 2010.

[23] J. Nocedal and S. J. Wright. *Numerical optimization.* Springer, 1999.

[24] J.-S. Pan, P. Hu, V. Snávsel, and S.-C. Chu. A survey on binary metaheuristic algorithms and their engineering applications. *Artificial Intelligence Review*, 56(7):6101–6167, 2023.

[25] H. Qin, R. Gong, X. Liu, X. Bai, J. Song, and N. Sebe. Binary neural networks: A survey. *Pattern Recognition*, 105:107281, 2020.

[26] M. Raghavachari. On connections between zero-one integer programming and concave programming under linear constraints. *Operations Research*, 17(4):680–684, 1969.

[27] R. T. Rockafellar and R. J.-B. Wets. *Variational analysis*, volume 317. Springer Science & Business Media, 2009.

[28] M. Shao and W.-K. Ma. Binary MIMO detection via homotopy optimization and its deep adaptation. *IEEE Transactions on Signal Processing*, 69:781–796, 2020.

[29] J. Shi and J. Malik. Normalized cuts and image segmentation. *IEEE Transactions on Pattern Analysis and Machine Intelligence*, 22(8):888–905, 2000.

[30] D. Sun, K.-C. Toh, Y. Yuan, and X.-Y. Zhao. SDPNAL+: A Matlab software for semidefinite programming with bound constraints (version 1.0). *Optimization Methods and Software*, 35(1):87–115, 2020.

[31] H. Wang, Y. Shao, S. Zhou, C. Zhang, and N. Xiu. Support vector machine classifier via $l_{0/1}$ soft-margin loss. *IEEE Transactions on Pattern Analysis and Machine Intelligence*, 44(10):7253–7265, 2021.

[32] P. Wang, C. Shen, A. van den Hengel, and P. H. Torr. Large-scale binary quadratic optimization using semidefinite relaxation and applications. *IEEE Transactions on Pattern Analysis and Machine Intelligence*, 39(3):470–485, 2016.

[33] S. Weerasinghe, T. Alpcan, S. M. Erfani, and C. Leckie. Defending support vector machines against data poisoning attacks. *IEEE Transactions on Information Forensics and Security*, 16:2566–2578, 2021.

[34] Z. Wen, D. Goldfarb, and W. Yin. Alternating direction augmented Lagrangian methods for semidefinite programming. *Mathematical Programming Computation*, 2(3):203–230, 2010.

[35] H. Wolkowicz, R. Saigal, and L. Vandenberghe. *Handbook of semidefinite programming: theory, algorithms, and applications*, volume 27. Springer Science & Business Media, 2012.

[36] B. Wu and B. Ghanem. $\ell_p$-box ADMM: A versatile framework for integer programming. *IEEE Transactions on Pattern Analysis and Machine Intelligence*, 41(7):1695–1708, 2018.

[37] X. Yang, Z. Song, I. King, and Z. Xu. A survey on deep semi-supervised learning. *IEEE Transactions on Knowledge and Data Engineering*, 35(9):8934–8954, 2022.

[38] G. Yuan and B. Ghanem. Sparsity constrained minimization via mathematical programming with equilibrium constraints. *arXiv preprint arXiv:1608.04430*, 2016.

[39] G. Yuan and B. Ghanem. An exact penalty method for binary optimization based on MPEC formulation. In *Proceedings of the AAAI Conference on Artificial Intelligence*, volume 31, 2017.

[40] Z. Zhang, T. Li, C. Ding, and X. Zhang. Binary matrix factorization with applications. In *Seventh IEEE International Conference on Data Mining (ICDM 2007)*, pages 391–400. IEEE, 2007.

[41] S. Zhou, L. Pan, N. Xiu, and H.-D. Qi. Quadratic convergence of smoothing Newton's method for 0/1 loss optimization. *SIAM Journal on Optimization*, 31(4):3184–3211, 2021.